Nano-Micro Letters
e-ISSN 2150-5551
CN 31-2103/TB
REVIEW
https://doi.org/10.1007/s40820-024-01629-5

Cite as
Nano-Micro Lett.
(2025) 17:149

Received: 24 September 2024
Accepted: 11 December 2024

Advances in Anion Chemistry in the Electrolyte Design for Better Lithium Batteries

Hecong Xiao[1], Xiang Li[1] ✉, Yongzhu Fu[1] ✉

HIGHLIGHTS

- The impact of anions on the interface is summarized, including forming a solid electrolyte interphase (SEI), repairing the damaged SEI, and modulate electric double layer.
- The influence of anions on the solvation structure is presented, including enhancing desolvation process of the Li-ions and the anti-oxidant property of the electrolyte.
- This review also emphasizes the important role of anions in enhancing battery safety through their flame-retardant properties, as well as their impact on energy density and power density by altering reaction pathways and accelerating reactions.

ABSTRACT Electrolytes are crucial components in electrochemical energy storage devices, sparking considerable research interest. However, the significance of anions in the electrolytes is often underestimated. In fact, the anions have significant impacts on the performance and stability of lithium batteries. Therefore, comprehensively understanding anion chemistry in electrolytes is of crucial importance. Herein, in-depth comprehension of anion chemistry and its positive effects on the interface, solvation structure of Li-ions, as well as the electrochemical performance of the batteries have been emphasized and summarized. This review aims to present a full scope of anion chemistry and furnish systematic cognition for the rational design of advanced electrolytes for better lithium batteries with high energy density, lifespan, and safety. Furthermore, insightful analysis and perspectives based on the current research are proposed. We hope that this review sheds light on new perspectives on understanding anion chemistry in electrolytes.

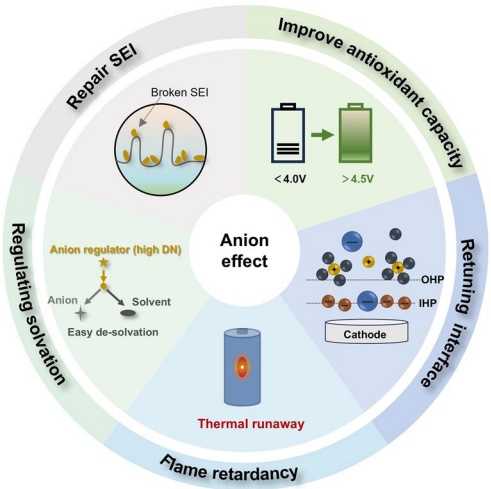

KEYWORDS Anion chemistry; Electrolyte; Interface; Solvation structure

1 Introduction

In today's energy field, lithium-ion battery (LIB) is one important electrochemical energy storage device, which has closely connected with our daily life. With the increasing requirement of sustainability, durable LIBs with long lifespans and safety are highly needed [1, 2]. The electrolyte, as one of the core components of batteries, bears the important responsibility of ensuring the stability and performance of the battery during the operation [3–5]. It is well known

✉ Xiang Li, xli@zzu.edu.cn; Yongzhu Fu, yfu@zzu.edu.cn
[1] College of Chemistry, Zhengzhou University, Zhengzhou 450001, People's Republic of China

Published online: 17 February 2025

that there are some typical electrolyte models, such as high-concentration electrolyte (HCE) [6–9], localized high-concentration electrolyte (LHCE) [10, 11], and weakly solvating electrolyte (WSE) [12–15], all of which focus on the solvents, such as decreasing the proportion of solvents and modifying the solvating ability of the solvents. Recently, the anions of Li-salts are applied for regulating the solvation structure of the electrolytes [16–18], which is a facile and effective strategy to achieve good electrochemical performance of LIBs. The anion is also an important component of the electrolyte, the effect of which, however, is often underestimated or overlooked.

Recent studies have shown that anions play multiple roles in interfacial electrochemistry and tuning the solvation sheath of Li-ions, which is very important for the formation of a solid electrolyte interphase (SEI) [19–23], the reaction kinetics at the electrode surface, and the stability of electrochemical performances [24–26]. Firstly, anions can decompose and help to form a solid SEI on the electrode surface [27–29], which is crucial for preventing solvents and salts from irreversible reactions at the electrode surface. Secondly, anions can participate in repairing the damaged SEI layer [30–32], thereby improving the stability of electrochemical performance and extending the electrode's lifespan. Additionally, anions can regulate the structure of the electric double layer (EDL) between the electrolyte and electrode surface [32–34], affecting the kinetic of charge transfer, ion transport, and distribution of species at interfaces. By adjusting the solvation environment, anions can also enhance the electrolyte's antioxidative and desolvation capabilities [35–38], thereby reducing side reactions in the electrolyte and improving battery cycle life. Furthermore, certain specific anions, such as halogens, possess flame-retardant properties, which can enhance battery safety [39, 40]. In recent years, Zhi et al. have thoroughly elucidated the critical role of anion chemistry in various energy storage devices, such as supercapacitors, cation rechargeable batteries, and metal–oxygen batteries [41]. Zhang et al. have emphasized the historical evolution and fundamental properties of salt anions [42]. The previous works provide profound insights into the critical role of anion chemistry in energy storage devices, while the design and functionalization of salt anions in new battery systems are not mentioned.

In this review, we will provide a detailed introduction to the key roles of anions, focusing on the precise design of anion structure and properties for better design of the LIBs (mainly focusing on the electrolyte). The typical anions we will introduce are displayed in Fig. 1, accompanied by the corresponding donor number (DN), which is a well-known parameter representing the coordination ability. By comprehensively understanding and fully utilizing the functions of anions in electrolytes, the electrochemical systems can be better designed and optimized, improving electrochemical performance, cycle life, and safety of the battery, which will make great contributions to promoting sustainable energy conversion and application. The following sections will delve deeper into the applications of anions in electrolytes, as well as their potential significance and future research directions.

2 Impact of Anions on the Interface

The SEI has a significant impact on the battery performance [43–47]. However, the formation of this interface is very complex and lacks in-depth research. The decomposition of anions plays a crucial role in the formation of the SEI layer [28, 48]. Before the formation of the SEI, a double layer and charge transfer are formed and processed at the interface, followed by chemical reactions and deposition of organic/inorganic components [49]. Next, we will explore how anions can adjust the interface from three aspects. The first is the anion-induced SEI formation, which mainly includes the formation of CEI at the cathode, the formation of AEI at the anode, as well as the formation of cathode electrolyte interphase (CEI) and anode electrolyte interphase (AEI) at the cathode and anode. The second is the detailed elaboration of how the anion repairs the SEI repair as well as the mechanism, and the last is the in-depth discussion of anion-regulated EDL.

2.1 Anion-Induced SEI

A SEI is derived from the decomposition of anions and solvents in the electrolyte. So, the electrolyte components play a curial role in the SEI properties [28, 50, 51]. The inorganic components (such as LiF and Li_3N) in SEI are usually considered good for the rigidity of this SEI and for a fast Li-ion transition [52]. It is known that inorganic components directly/indirectly come from the anions. Therefore, this section focuses on the anion-induced SEI, discussing the effect of anions on the formation of AEI, CEI, and both the AEI and CEI.

https://doi.org/10.1007/s40820-024-01629-5

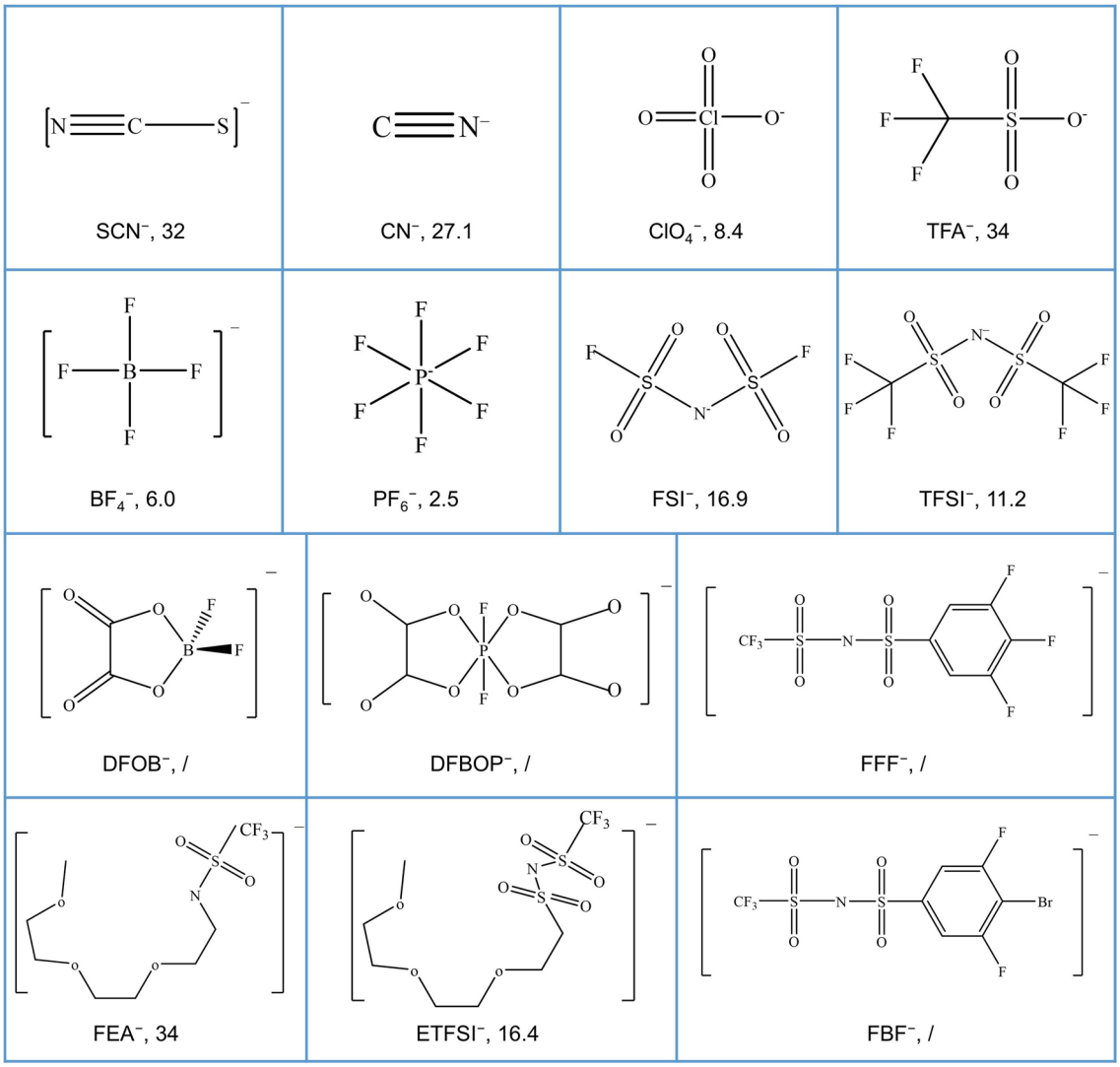

Fig. 1 The structures of the typical anions involved in this review, together with the DN values

2.1.1 Anion-Induced AEI

From the anode side, the application of lithium bis(fluorosulfonyl)imine (LiFSI)-based carbonate electrolytes (1 M LiFSI dissolved in ethylene carbonate (EC) and dimethyl carbonate (DMC) (1:1 v/v)) in LIBs has been reported to offer better cycling performance than traditional $LiPF_6$-based electrolytes [27]. This improvement is attributed to FSI^-, which contributes to forming a dense AEI film that can protect the graphite anode. Zhang et al. proposed a dual-salt electrolyte consisting of 0.8 M LiFSI and 0.2 M lithium difluoro(oxalato)borate (LiDFOB) in fluoroethylene carbonate (FEC)/tetra (ethylene glycol) dimethyl ether (TEGDME) [53]. In this electrolyte, the addition of LiDFOB effectively prevents the dissolution of Fe from the $LiFePO_4$ cathode [54]. Moreover, both LiFSI and FEC facilitate the formation of a thermally stable AEI on the surface of the graphite anode, particularly at high temperatures (70 °C), significantly enhancing the safety of the batteries.

In addition to the formed AEI on the graphite, Mullins et al. utilized various lithium salts (e.g., $LiPF_6$, LiTFSI, LiFSI, and LiDFOB) to achieve high stability lithium anodes based on tetrahydrofuran (THF) electrolyte systems [25]. The anions preferentially decompose instead of organic solvents, producing inorganic-rich AEI. The LiDFOB-based electrolyte has the lowest viscosity (1.10 mPa s),

highest Li^+ transport numbers, and highest ionic conductivity (16.1 mS cm^{-1}) among the electrolytes based on different Li-salts. Moreover, the AEI film generated by the decomposition of $DFOB^-$ is the thinnest, which may be the reason that the LiDFOB electrolyte offers an excellent cycling performance (over 3200 h) in a symmetrical cell at a current density of 0.5 mA cm^{-2} (Fig. 2a). Dahn applied LiDFOB and $LiBF_4$ as dual-salt carbonate electrolyte additives in an anode-free lithium pouch cell, which maintains 80% capacity retention after 90 cycles [55]. However, the stability of the cell with single-salt electrolyte ($LiBF_4$) drops below 80% retention in less than 15 cycling cycles (Fig. 2b). The AEI film established within the dual-anions contains a significant quantity of LiF, which promotes the uniform deposition of lithium. In addition to some commonly used anions, there are also some new lithium salts (anions) that can also modify the interface. For example, Liu et al. developed an asymmetric trihalogenated aromatic lithium salt, namely LiFFF and LiFBF [56] (Fig. 2c), as a single conductive lithium salt in polymer electrolytes for all-solid-state lithium batteries. The electrolytes with LiFFF and LiFBF not only possess high Li^+ transport number (Fig. 2d) but also generate a good AEI on the negative electrode surface. Particularly, LiFBF induces a LiF/LiBr mixed AEI that can passivate the lithium metal anode because LiF exhibits a high Young's modulus and high surface energy to homogenize Li^+ flux, while the activation energy for ion transport in the interphase of LiBr is reduced by approximately three times compared to LiF. Therefore, the interface stability of the anode has been significantly enhanced. As a result, Li||Li symmetric cell can stably cycle for over 1200 h without short circuits. And Li||$LiFePO_4$ batteries can work for 1200 cycles at rate of 1 C, demonstrating excellent electrochemical performance.

Like lithium batteries, anion chemistry has also been used in sodium batteries to regulate the interphase. Chen et al. constructed a unique uniformly dispersed high conductivity inorganic-rich AEI by introducing self-sacrificial LiTFSI into sodium-based electrolytes (0.75 M $NaClO_4$ in FEC/PC (propylene carbonate)) [57]. The reduction between LiTFSI and FEC promotes the formation of inorganic SEI (Fig. 2e). Among them, highly conductive inorganic substances provide fast ion transport domains and high-throughput nucleation sites for Na^+, which is conducive to the rapid deposition of sodium. The AEI derived from LiTFSI and FEC resulted in high capacity retention of 89.15% in the Na||$Na_3V_2(PO_4)_3$ battery after 1000 cycles at an ultra-high rate of 60 C. Xia et al. introduced $NaNO_3$ into the ester-based electrolyte (1 M $NaClO_4$ in EC/PC (1:1) with 2% FEC) to control interface chemistry and AEI properties [58]. Due to the strong solvating ability of NO_3^-, the NO_3^- occupies the solvation shell of Na^+ and decomposes instead of other anions. With the help of FEC additives, a stable AEI containing Na_3N and NaF is generated on Na metal surface. With this advantageous AEI, the lifespan of electrodes based on transition metal sulfides (FeS@NS-C) can be markedly prolonged by more than 2000 cycles (Fig. 3a).

2.1.2 Anion-Induced CEI

Zhou et al. introduced Li_2O as a preloaded sacrificial agent mixed with $LiNi_{0.8}Co_{0.1}Mn_{0.1}O_2$ cathode to provide an additional lithium source to offset the irreversible loss of lithium for long-term cycling of batteries [5]. In situ surface-enhanced Raman spectroscopy (SERS) studies have shown that the O_2^- anions released through the oxidation of Li_2O are synergistically neutralized by the fluorinated ether additives, forming a LiF-based CEI, which passivates the surface of the cathode and inhibits the deleterious oxidative decomposition of the solvent. As a result, a long-life 2.46-Ah anode-free pouch battery was developed with a gravimetric energy density of 320 Wh kg^{-1} retaining 80% capacity retention after 300 cycles (Fig. 3b). Xie et al. reported a strategy by adding a trace amount of LiDFOB to the NCM811 cathode to form a high-voltage solid-state lithium metal batteries (LMBs) [59]. A CEI layer consisting of LiF and $Li_xBO_yF_z$ was in situ constructed through the synergistic decomposition of $DFOB^-$ and $TFSI^-$ from ionic liquids, which effectively suppressed the occurrence of side reactions and cracks of NCM particles during the high-voltage cycles. Therefore, the solid-state lithium battery with CEI-protected NCM811 exhibits an initial specific capacity of 190.7 mAh g^{-1} at a high cut-off voltage of 4.5 V at rate of 0.1C and capacity retention of more than 80% at 60 °C for 100 cycles, while the capacity of the cell without adding LiDFOB at a high voltage of 4.5 V dropped to 48.3% after only 50 cycles (Fig. 3c). Wu et al. added a trace of $LiPF_6$ (0.05 M) additive to a dual-salt (LiTFSI-LiBOB) carbonate electrolyte, vastly improving the cycle stability of LMBs (Fig. 3d). The addition of $LiPF_6$ serves two purposes: the one is that it can stabilize the Al current collector, suppressing the Al corrosion. More significantly, a small amount of

https://doi.org/10.1007/s40820-024-01629-5

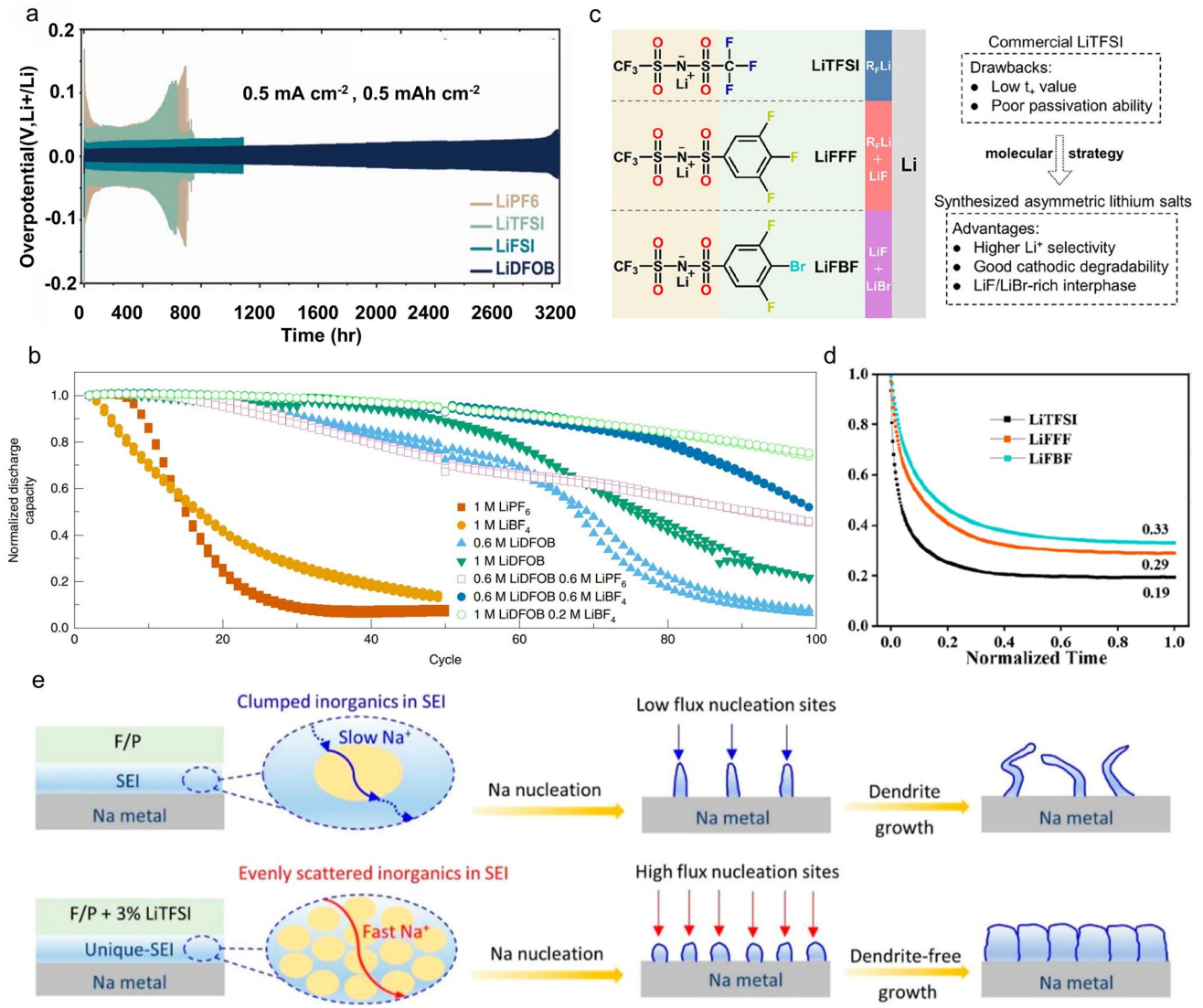

Fig. 2 **a** Long-term stability testing of Li||Li symmetrical cells using various THF-mixed electrolyte systems under low current density conditions [25]. Copyright 2023, Wiley–VCH GmbH. **b** The relationship between cycle number and capacity retention for anode-free pouch cells with various lithium salt electrolytes [55]. Copyright 2019, Springer Nature. **c** Two novel lithium salts with structures and film formation properties based on LiTFSI. **d** Li^+ transference number of the polymer electrolytes with different Li-salts [56]. Copyright 2023, American Chemical Society. **e** Schematic diagram illustrating the SEI formation in electrolytes with and without LiTFSI [57]. Copyright 2023, American Chemical Society

$LiPF_6$ additively changed the component of the SEI. The improved interfacial stability facilitates the continuous operation of LMBs even at high charge current densities [60].

2.1.3 Anion-Induced AEI and CEI

Zheng et al. reported a novel electrolyte additive of potassium selenocyanate (KSeCN) for LMBs [61]. The additive has a high HOMO (the highest occupied molecular orbital) and a low LUMO (the lowest unoccupied molecular orbital), allowing it to preferentially decompose during battery charging and discharging processes. It forms a Se-containing protective layer on the surface of the $LiCoO_2$ (LCO) cathode and lithium metal anode, thereby inhibiting the decomposition of the electrolyte at the cathode/anode interface. The functional additive can retard the dissolution of transition metal ions and significantly improve the stability of

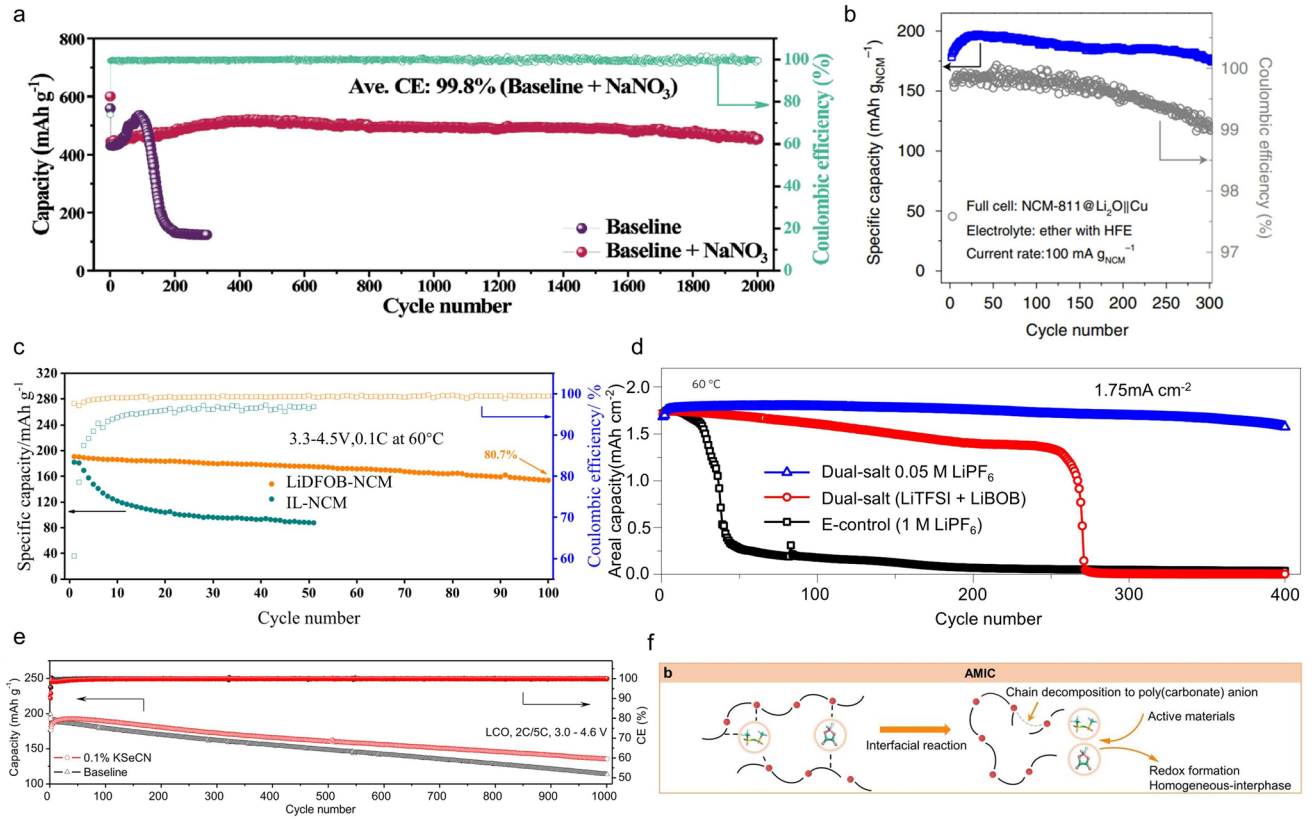

Fig. 3 **a** Cycle performance of the Na||FeS@NS-C half cells using baseline and optimized electrolytes at 1.0 A g^{-1} [58]. Copyright 2023, Wiley–VCH GmbH. **b** Discharge capacity hysteresis plotted against cycle number [5]. Copyright 2021, Springer Nature. **c** Cycle performance in the voltage range of 3.3–4.5 V with and without a dual-salt composite cathode [59]. Copyright 2023, Elsevier. **d** Cycling performance of Li||NMC batteries with different electrolytes at 60 °C [60]. Copyright 2017, Springer Nature Limited. **e** Cycling performance of Li||LCO batteries using baseline and optimized electrolytes at a 2C charge rate and a 5C discharge rate [61]. Copyright 2022, American Chemical Society. **f** Schematic representation of the interfacial decomposition mechanism of anion-modulated ion conductor (AMIC) [63]. Copyright 2024, Wiley–VCH GmbH

the lithium metal anode. Compared with Li||LCO battery with traditional ester electrolytes, the battery with 0.1 wt% KSeCN additive can maintain stable cycling at a high cut-off voltage of 4.6 V (Fig. 3e). Xia et al. regulated the carbonate-based electrolyte through the multi-functional additive lithium difluorobis(oxalato) phosphate (LiDFBOP) [62]. Theoretical calculation and physical and chemical characterization confirmed that $DFBOP^-$ as film forming agent, preferentially reacted on both sides of the $Na_3V_2(PO_4)_2F_3$ cathode and Na anode to form a stable and strong interphase (CEI/AEI). At the same time, Li^+ regulates the stability of the electrolyte by regulating the solvation structure and suppresses dendritic growth through electrostatic shielding.

Fan et al. proposed a strategy called anion-modulated ionic conductor (AMIC) to address the problem of uneven electrolyte–electrode interface stability in solid-state LMBs [63]. By employing two types of anions ($DFOB^-$ and $TFSI^-$), the decomposition behavior of the polymer chain segments at interphase was altered, converting poly (vinylene carbonate) (PVC) to polycarbonate anion, which promotes the uniform deposition of lithium ions (Fig. 3f). Specifically, the polymer chain segments shift to a more favorable entropic globular conformation under the influence of anions (coordination properties of carbonyl groups). In addition, the spherical conformation exposes more lithium-ion binding sites, improving the interchain transfer of lithium ions [64]. Consequently, the electrolyte exhibits high ionic conductivity of 1.78×10^{-4} S cm^{-1} (at 60 °C), high Li^+ transport number ($t_{Li}{}^+ = 0.67$), and a broader electrochemical window (upon to 4.8 V). Furthermore, the two anions form stable SEI on both sides. The AEI maintains uniform deposition of Li-ions and inhibits dendric Li growth, while

 https://doi.org/10.1007/s40820-024-01629-5

the CEI preserves the structural stability of the cathode. Li||$LiNi_{0.8}Co_{0.1}Mn_{0.1}O_2$ cell maintains about 85% capacity retention and the coulombic efficiency is > 99.8% in 200 cycles at a charge cut-off voltage of 4.5 V.

2.2 Repairing SEI by Anions

The failure of LMBs is caused by various reasons, including the growth of dendritic lithium, accumulation of inactive lithium (also known as dead lithium), and unstable SEI [65, 66]. The presence of dead lithium is the primary cause of the performance degradation in LMBs [67]. There is an urgent need for a basic solution for recycling dead lithium to stabilize LMBs [68].

Tao et al. proposed a lithium reduction method based on a series of iodine redox reactions primarily involving I_3^-/I^- process [69]. Using iodine as a biochar capsule host, they found that the I_3^-/I^- redox takes place spontaneously. As shown in Fig. 4a, LiI, as an intermediate product, functions as a carrier for the lithium element (Li-vehicle), while $LiIO_3$ as a carrier for the oxygen element (O-vehicle). The reaction can effectively activate "dead lithium" and facilitate the transport of Li_2O within the "dead SEI". Meanwhile, Frontline molecular orbital theory calculations confirm that iodine species exhibit a higher electron affinity compared to solvent molecules and anions (of Li-salts) in the electrolyte, making iodine preferentially react with lithium metal, thereby inhibiting the decomposition of the electrolyte. With this design, a full battery assembled with a Li@ICPC (iodine-carbonized porous conidial powder) anode and $LiFePO_4$ (LFP) cathode can even maintain 1000 cycles with capacity retention of 80% under a low negative/positive (N/P) ratio of 2.5 (Fig. 4b). Zhang et al. also recovered inactive lithium by using an I_3^-/I^- redox pair initiated by stannic iodide (SnI_4) [31]. The I_3^- facilitates the conversion of inactive Li into soluble LiI, which then migrates toward the cathode. Following this, the delithiated cathode oxidizes LiI, regenerating I_3^- through cathode lithiation. Consequently, inactive Li is continuously reclaimed during the battery cycling. The viability of this strategy for recycling inactive lithium has been successfully demonstrated in Li||$LiNi_{0.5}Co_{0.2}Mn_{0.3}O_2$ batteries, resulting in a doubled lifespan (Fig. 4c). In addition, the feasibility of the method was further verified by comparing the morphology of lithium after cycling (Fig. 4d, e). This method is also applicable to solid polymer electrolytes (SPE). Tao et al. applied a trace amount of I_2 into polyethylene oxide (PEO) electrolytes to establish stable interphase on lithium metal surfaces, thus ensuring prolonged battery cycling [70]. The I_3^- from iodine additives can coordinate with the –COC– bond of PEO, thereby improving the ionic conductivity of the SPE. In addition, I_3^- can spontaneously react with dead Li and Li_2O, leading to the formation of a dense and uniform iodine-doped SEI layer in situ on the lithium anode surface, ultimately reducing interface resistance and inhibiting dendrite growth. Li et al. synthesized iodine-doped polyacrylonitrile (I-PAN) negative electrode materials using a low-temperature calcination method, demonstrating an excellent fast-charging performance of lithium/sodium-ion batteries [71]. The iodine of the I-PAN backbone is prone to nucleophilic substitution reaction with the PF_6^- in the electrolyte to form I^-. Raman/NMR/molecular dynamics simulations show that I^- readily enters the solvated inner layer of Li^+ and promotes its desolvation process. Under fast-charging conditions, the dead lithium formed on the negative electrode can be reused through reversible I^-/I_3^- redox reactions to compensate for the lithium loss. Therefore, I-PAN enables rapid bulk/interface Li^+ diffusion kinetics, accelerated desolvation processes, formation of SEI rich in LiF/LiI, and reuse of dead lithium. When discussing the issue of dead lithium recovery, the stability of the SEI and its crucial role in the lithium deposition and stripping processes cannot be overlooked. The formation of dead lithium is closely related to the failure of the SEI, and the success of dead lithium recovery also depends on effective SEI repair. By repairing the SEI, lithium dendrite growth can be suppressed, which in turn reduces the generation of dead lithium. Therefore, dead lithium recovery and SEI repair are not only interrelated but also collaborative improve the cycling stability and lifespan of lithium metal batteries. Next, we will further explore the specific mechanisms of anion-based SEI repairing and its applications in electrolyte design.

Specific Li-salts can also be used for self-repairing of SEI. An asymmetric Li-salt, lithium 1,1,1-trifluoro-N-[2-[2-(2-methoxyethoxy) ethoxy)] ethyl] methanesulfonamide (LiFEA) was designed by Liu et al. (Fig. 4f), which has a pseudo-crown ether-like folded molecular geometry and gives carbonate electrolytes, high large apparent donor number and Li^+ transference number [72]. More importantly, during the SEI construction process, the anion can dissolve unwanted organic species (for example,

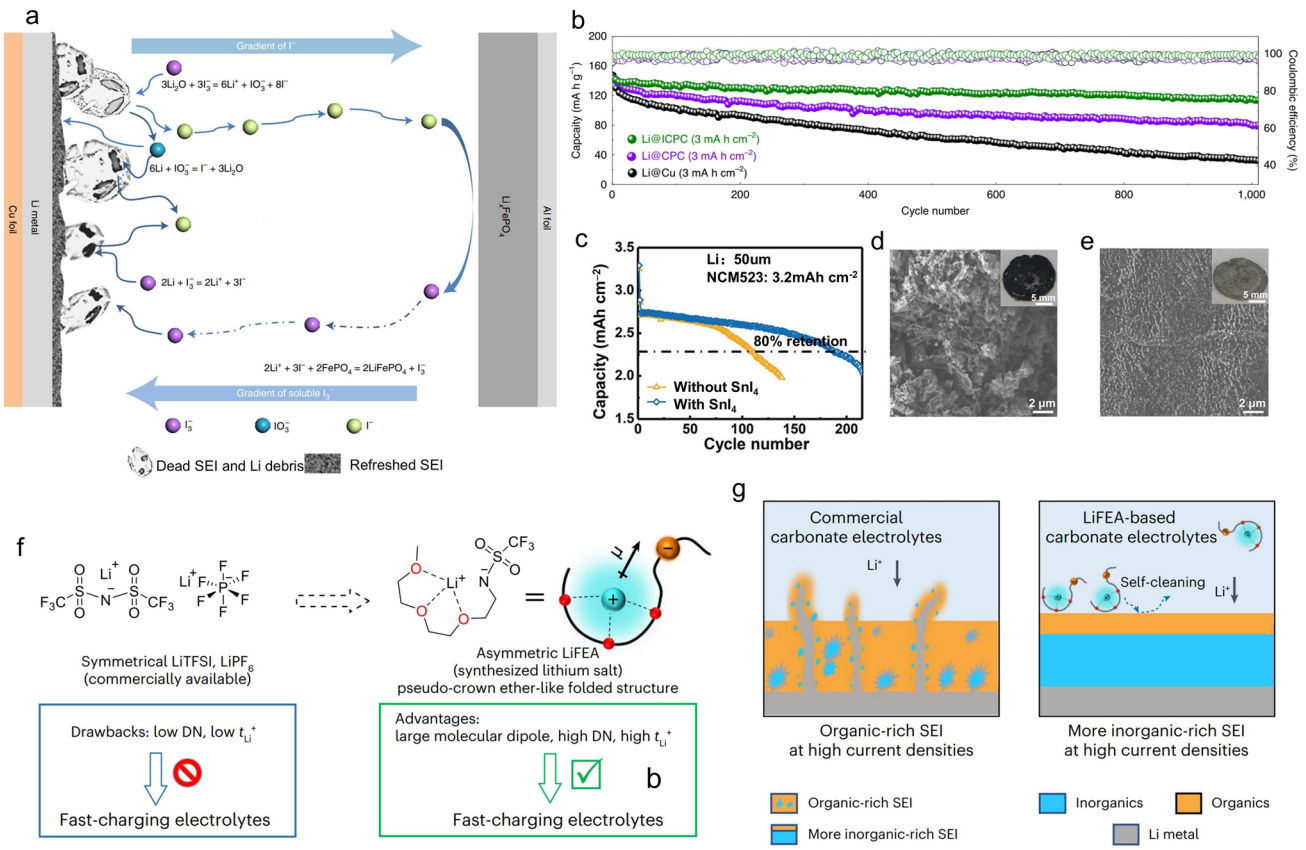

Fig. 4 **a** Schematic diagram of the mechanism for lithium restoration based on iodine redox cycling. **b** Cycling performance of Li@ICPC, Li@CPC and Li@Cu anodes with a low N/P ratio of 2.5 in LFP full cells at 1C [69]. Copyright 2021, Springer Nature. **c** Cycling performance of Li||NCM523 without SnI_4 and with SnI_4. **d** SEM image of Li foil after cycling in $LiPF_6$-DMC/FEC electrolyte. **e** SEM image of cycled Li foil after soaking in $LiPF_6$-DMC/FEC electrolyte with 4.0 mM SnI_4 additive [31]. Copyright 2021, Wiley–VCH GmbH. **f** Comparison of LiFSI, $LiPF_6$ with LiFEA. **g** Schematic representation of LiFEA-based electrolytes enabling a more inorganic-rich SEI layer and dendrite-free Li deposition through self-cleaning action compared to commercial carbonate electrolytes [72]. Copyright 2023, Springer Nature

$ROCO_2Li$, $-(CH_2CH_2O)_n-$) formed in carbonate electrolytes (Fig. 4g), leading to the gradual enrichment of inorganic species in the SEI. They combined quartz crystal microbalance analysis with electrochemical methods (EC-QCM) to monitor changes in SEI quality during immersion treatment. The SEI mass decreased by 25.7 μg, which is three times higher than that of the blank case (1 M $LiPF_6$ EC/DEC (v/v = 1:1)). This finding is consistent with the X-ray photoelectron spectroscopy (XPS) and time-of-flight secondary ion mass spectrometry (TOF–SIMS) results from the soaking experiment. This unique self-cleaning mechanism helps to generate dense and uniform SEI rich in inorganic substances. Based on LiFEA-based carbonate electrolyte, the Li||NCM811 battery exhibits outstanding cycling performance. The pouch cell maintained 81% capacity retention after 100 cycles (charge: 0.4C, discharge: 1C). In contrast, the blank cell survived only 50 cycles under identical conditions. These results indicate that LiFEA-based carbonate electrolyte has promising potential for widespread application in high-performance LMBs. However, through in-depth research into the physicochemical properties of LiFEA, it has been discovered that the excessively high donor number (DN) of FEA^- can lead to high reactivity and poor compatibility with some solvents (such as FEC). Therefore, to address this issue, a new lithium salt lithium, 2-[2-(2-methoxy ethoxy)ethoxy] ethanesulfonyl(trifluoromethanesulfonyl) imide (LiETFSI) has been introduced based on FEA^- by incorporating sulfonyl groups [73]. Electrolytes containing LiETFSI in carbonate solvents not only ensure high conductivity but also exhibit a higher Li^+ transference number ($t_{Li}{}^+ \approx 0.8$) with a moderate DN. The anion facilitates the dissolution of

 https://doi.org/10.1007/s40820-024-01629-5

oxygen-containing organic compounds in the SEI while reducing the dissolution of inorganic components such as LiF, confirmed by XPS and TOF–SIMS. Consequently, the electrolyte establishes a SEI interface with a lower impedance rich in inorganic components. The advanced LiETFSI electrolyte (with $LiNO_3$) enhances the CE to 99.0%, indicating a high reversibility of the Li plating/stripping process. In comparison, the CE with advanced LiFEA electrolyte only reaches 96.6%, and the addition of FEC does not make a big difference due to the poor compatibility between LiFEA and FEC. Taking advantage of the film-forming properties of FSI^- and the photopolymerization properties of vinyl, Wang et al. crosslinked the ionic liquid 1-vinyl-3-methylimidazolium bis(fluorosulfonyl)imide (VMI-FSI) with poly(ethylene oxide), to form a self-healing membrane with the FSI^- group as the repair agent [74]. When they encounter lithium metal, the FSI^- groups are chemically decomposed into LiF and Li_3N, which assist in forming SEI on lithium metal and repairing SEI in the cracks lacerated by lithium dendrite. Furthermore, the FSI^- anions exchanged from the film are electrochemically decomposed to inorganic components to strengthen the SEI. This self-healing layer demonstrated excellent performance in Li||LCO cells which are stably operated for 500 cycles with the retention rates of 81.4% and the average coulombic efficiency of 99.97% at 4.5 V. The strategies hold significant potential for applications in the field of LMB. Although researchers have proposed methods based on iodine-based redox reactions and designing self-healing molecules to repair dead lithium and SEI, in practical applications, these approaches may encounter challenges such as stability and cost issues. Therefore, it remains imperative to consider how to address such a challenge.

2.3 Anion-Modulated EDL of the Cathode

The electrochemical reactions take place in the EDL, actually in the inner Helmholtz plane (IHP), and therefore, the evolution of EDL at the electrode/electrolyte interface is very critical [74, 75]. The characteristics of this layer on the cathode surface can be modulated by the anions due to the electric field in the IHP. Herein, the interface properties of the cathode have a directly relationship with the anions. The anion in the IHP that can regulate the CEI formation process is optimal, so as to prevent excessive electrolyte consumption, especially for the ether electrolytes. Kang et al. proposed an electrolyte design strategy to enhance the oxidation stability of a dilute ether electrolyte (1 M LiTFSI in DME) using trace amounts of nitrate additive (50 mM NO_3^-) [33]. The combined experiments and molecular dynamics simulations reveal that a novel interface is formed by the aggregation of NO_3^- anions in the IHP, thereby eliminating solvent molecules at the interface and inhibiting the oxidative decomposition of solvent molecules (Fig. 5a). This adsorption behavior is crucial for expelling solvent molecules at the interface and regulating the electrochemical environment of the interface. As a result, the ether electrolyte can endure a high voltage of 4.4 V. Meanwhile, Liu et al. also applied NO_3^- additives to ether-based electrolytes (1 M LiFSI in DME) to construct a dynamic and highly stable EDL at the CEI [34]. This non-traditional EDL is filled with nitrate ions, enhancing the oxidation stability of ether-based electrolytes and passivating the decomposition of the electrolyte. Specifically, NO_3^- can quickly migrate to the cathode interface under the electric field during the battery charging, forming a "supramolecular dynamic network structure" with Li^+ and solvents (Fig. 5b). With the improved EDL, LMBs utilizing conventional ether electrolytes ($\leq$ 1 M) exhibit excellent performance, such as high cut-off voltage up to 4.5 V (vs. Li/Li^+), excellent ultra-fast cycling performance (Li||NCM811, 5 C, 90% capacity retention after 700 cycles), and ultra-low temperature performances (86 mAh g^{-1} at –91 °C). In addition, Zhang et al. used trace amounts of $LiNO_3$ and CuF_2 in ether-based electrolytes to modify the structure of the EDL [74]. They verified that NO_3^- is more easily adsorbed as the dominant anion in the IHP compared with FSI^- (Fig. 5c). The special structure ensures a good SEI containing nitrogen oxides, inducing spherical growth of metallic lithium. The lifespan of Li||$LiFePO_4$ cell (capacity retention of 92.5% after 700 cycles) is at least 12 times than that of the batteries without the additives.

In addition to applying NO_3^-, Lu et al. proposed a specific adsorption-oxidation (Ad-O) strategy. The formation of the CEI is determined by utilizing trace amounts of 1,3,6-hexanetricarbonitrile (HTCN) and LiDFOB (Fig. 5d) [76]. The HTCN and $DFOB^-$ compete with the primitive carbonates and PF_6^- for adsorbing at the cathode surface by specific electron-rich groups to form novel structures within the IHP, thereby "squeezing" the most primitive compositions. This strong interaction masks the active sites on the surface of the

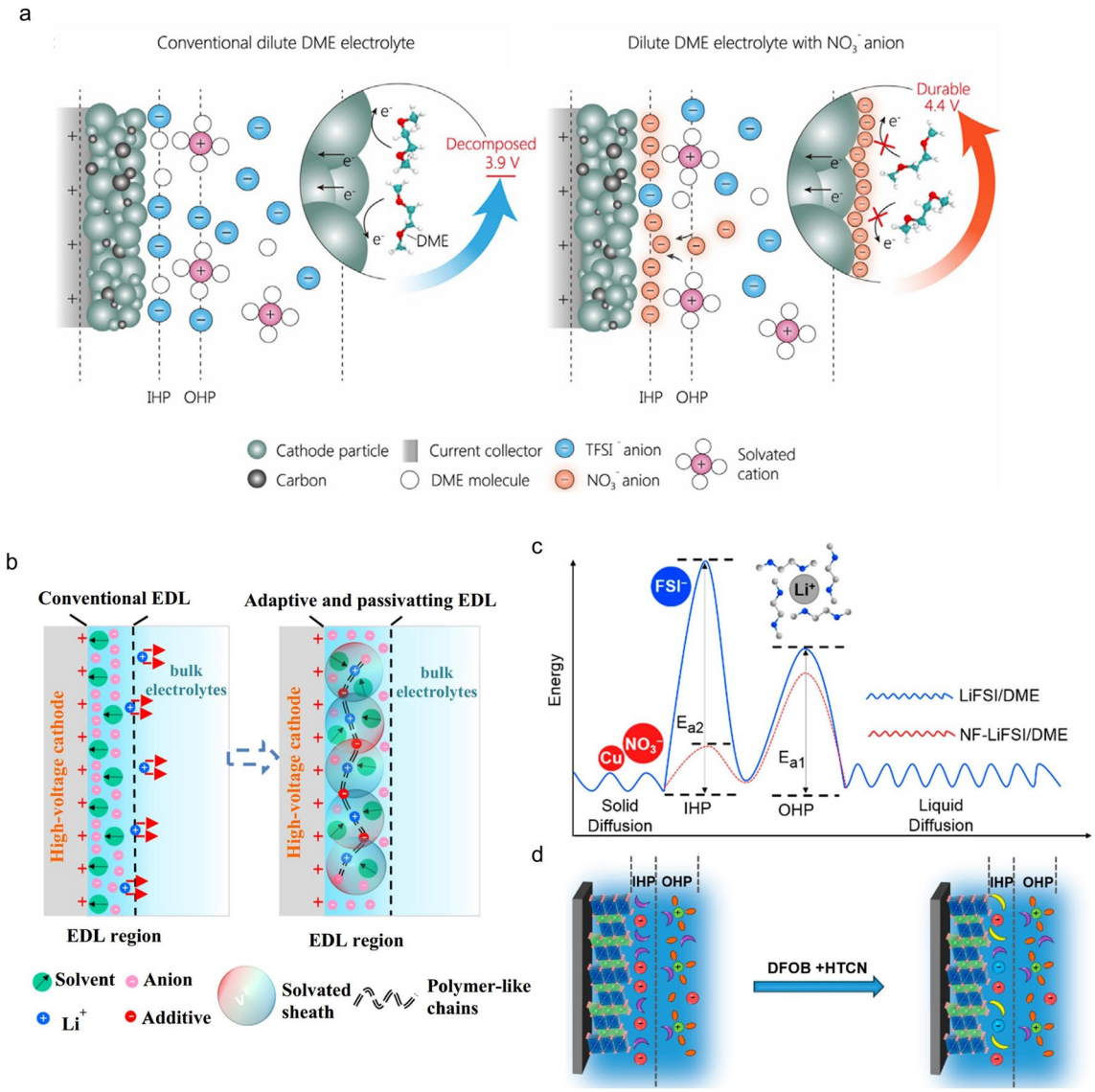

Fig. 5 **a** Schematic representation of the mechanism for improving and optimizing the interface by adding nitrate ions to the traditional ether-based dilute electrolyte [33]. Copyright 2022, Elsevier. **b** Proposed mechanism for constructing a dynamic high-voltage resistance EDL [34]. Copyright 2022, Springer Nature. **c** Correlation between the energy barrier of Li^+ and the specific adsorption in the inner Helmholtz plane (IHP) and outer Helmholtz plane (OHP) [74]. Copyright 2019, American Chemical Society. **d** Schematic illustration of IHP changes after adding additives of HTCN and LiDFOB [76]. Copyright 2023, American Chemical Society

cathode, preventing a weak CEI produced by the dehydrogenation and oxidation of traditional carbonates. After initial cycles, a double-layer CEI was formed with LiF as the inner layer and organic-rich B − F/ − CN component as the outer layer, further protecting the electrolyte and the cathode from decomposition and crystal degradation, respectively. This cooperative effect makes the cathode maintain stable cycling performances even under high voltages of 4.6 V and elevated temperatures of 60 °C.

Chen et al. improved the storage performance of $Na_{2.26}Fe_{1.87}(SO_4)_3$ by exposing the (112) plane to constitute a robust CEI [77]. The special plane promotes the adsorption of the ClO_4^- and FEC, forming an inorganic-rich Na^+ conductive interphase at the cathode. As a result, when tested in combination with a presodiated FeS/carbon-based negative electrode in laboratory-scale single-layer pouch cell configuration, the $Na_{2.26}Fe_{1.87}(SO_4)_3$-based positive electrode enables an initial discharge capacity of about 83.9 mAh g^{-1}.

https://doi.org/10.1007/s40820-024-01629-5

Researchers have also proposed the application of lithium trifluoroacetate (LiTFA)-$LiNO_3$ dual-salt additives in $LiPF_6$-based carbonate electrolytes [78]. By constructing a thermodynamically favorable EDL structure on the positive electrode interface, the kinetics of interfacial reactions have been significantly accelerated. This greatly enhances the thermodynamic compatibility between the carbonate electrolyte and the high-voltage layered transition metal oxide positive electrode. Specifically, the use of hygroscopic LiTFA as a dual-functional additive inhibits the hydrolysis of $LiPF_6$ and promotes the dissolution of $LiNO_3$ in the carbonate electrolyte. Even after exposure to humid air for 12 h, the capacity retention of 78.3% can be achieved after 200 cycles in Li||NCM523 batteries using a newly proposed moisture-resistant carbonate electrolyte.

3 Influence of Anions on the Solvation Structure

The solvation structure refers to the arrangement formed when solute ions are surrounded by solvent molecules in an electrolyte solution [79]. This structure directly affects the movement and reactivity of ions in the solution [80]. Solvent molecules interact with solute ions through electrostatic interactions, hydrogen bonding, or coordinate bond, resulting in the formation of a solvation shell [28]. The composition, structure, and physicochemical properties of SEI largely depend on the solvation structure of the electrolyte. To modulate the solvation chemistry in liquid electrolytes, it is imperative to comprehend the interplay between ions and solvents. These interactions are intricately linked to regulating interface stability, expanding the electrochemical stable potential window, controlling kinetics, and suppressing side reactions within batteries.

3.1 Anion-Regulated Stable Interface

As discussed above, SEI is formed through the decomposition of the anions and solvents. Therefore, the SEI properties can be controlled by tuning the electrolyte components (solvation structure). Zhang et al. proposed that when the anion is coordinated with the Li^+-solvent complex, the LUMO energy level of the solvent becomes higher and that of the anion becomes lower [81]. This indicates that the participation of anions in the Li^+-solvent sheath not only improves the reduction stability of the solvent but also promotes the reduction of the anions. Anions in the solvation sheath readily accept electrons and undergo a reduction process, leading to the formation of an inorganic-rich AEI. The use of anions with high DN values is often an effective strategy for modulating the solvation sheath [82]. As an example, $LiNO_3$ is also a well-known film-forming agent with a high DN value (22 kcal mol^{-1}) and is usually used in electrolytes as an additive [15, 83–85]. Introducing NO_3^- into the electrolyte can obtain a solvation structure rich in NO_3^- while poor in solvents, inducing a large number of contact ion pairs (CIPs) and ion aggregates (AGGs). The solvation structure regulated by NO_3^- dominates the formation of inorganic-rich SEI [86].

Chen et al. introduced $LiPF_6$ and $LiNO_3$ as dual-salt additives in an electrolyte of LiTFSI in DOL/DME and obtained a high CE of 99.3% and long cycling stability of the Li||LFP ($N/P = 2$) cell [87]. The enhancement of the cell could be attributed to the formation of a good SEI that contains both inorganic and organic components. Li et al. developed an optimized ether-based electrolyte (OEE) by adding $LiNO_3$ and vinylene carbonate (VC) [88]. This electrolyte (1 M LiDFOB and 0.5 M $LiNO_3$ in pure DME with 5 vt% VC) provides high lithium-ion conductivity (11.52 mS cm^{-1} at 20 °C) and high voltage stability (4.4 V). $LiNO_3$ and VC can enter the inner solvation shell and preferentially participate in the film-forming process at the electrode surface, resulting in the formation of a unique organic–inorganic bilayer interfacial protective layer. This protective layer effectively suppresses electrolyte side reactions and enhances electrode stability. Consequently, the 4.4 V NCM811 full cells assembled with the OEE exhibit stable cycling performance at both room temperature (Fig. 6a) and low temperatures (− 20 °C).

The solubility of most nitrates in carbonate electrolytes is rather limited, so in previous work, Lewis acid was used as an electron-rich NO_3^- acceptor to decompose $LiNO_3$ clusters [89, 90]. For example, our previous work used $Cu(NO_3)_2$ as an additive to regulate the solvation structure of 1 M $LiPF_6$ in EC/DEC (1:1, vol%) electrolyte. Since the electrostatic interaction of Li^+ with NO_3^- is stronger than with PF_6^-, NO_3^- entered the solvation sheath of Li^+, which can be demonstrated by NMR and Raman results. XPS results showed that the inorganic-rich components in the SEI, which is favorable for the Li conduction and the stability of the SEI. The Li||NCM811 cell exhibits capacity retention as high

as 95.73% after 600 cycles at room temperature (Fig. 6b) and outstanding cycle performance for wide temperatures (0 and 50 °C). Similarly, we have previously proposed a new strategy to promote nitrate dissolution in ester electrolytes via crystalline H_2O. As a typical case, the solubility of $In(NO_3)_3$-$6H_2O$ in commercial ester electrolyte is 0.2 M, which improves the cycling stability of LMB [91]. The additive can promote the generation of stable SEI with the inorganic-rich components on the LMA surface, inhibiting the formation of lithium dendrites, which is further demonstrated by the XPS results. After 300 cycles, the Li||NCM811 cell with $In(NO_3)_3$ additive has a capacity retention of 90.0% and an average CE of 99.3% (Fig. 6c), while the blank one only delivers capacity retention of 57.7%, with a low CE of 95.6%.

In addition to nitrate ions, there are other ions beneficial for the film formation. Zheng et al. designed an electrolyte composed of LiFSI in DME and 1,1,2,2-tetrafluoroethyl 2,2,3,3-tetrafluoropropyl ether (TTE) (3: 2 by molar) with 0.1 M $LiPF_6$ (L-LDT) [92]. Based on Ab-initio molecular dynamics (AIMD) simulations along with the corresponding radial distribution functions (RDFs) analysis, a high density of Li-F peaks was observed at 1.92 Å (Fig. 6d). This provides direct evidence of PF_6^- involvement in the main solvation sheath. Meanwhile, a stronger Li-O_{DME} peak indicates that the interaction between DME and Li^+ is further

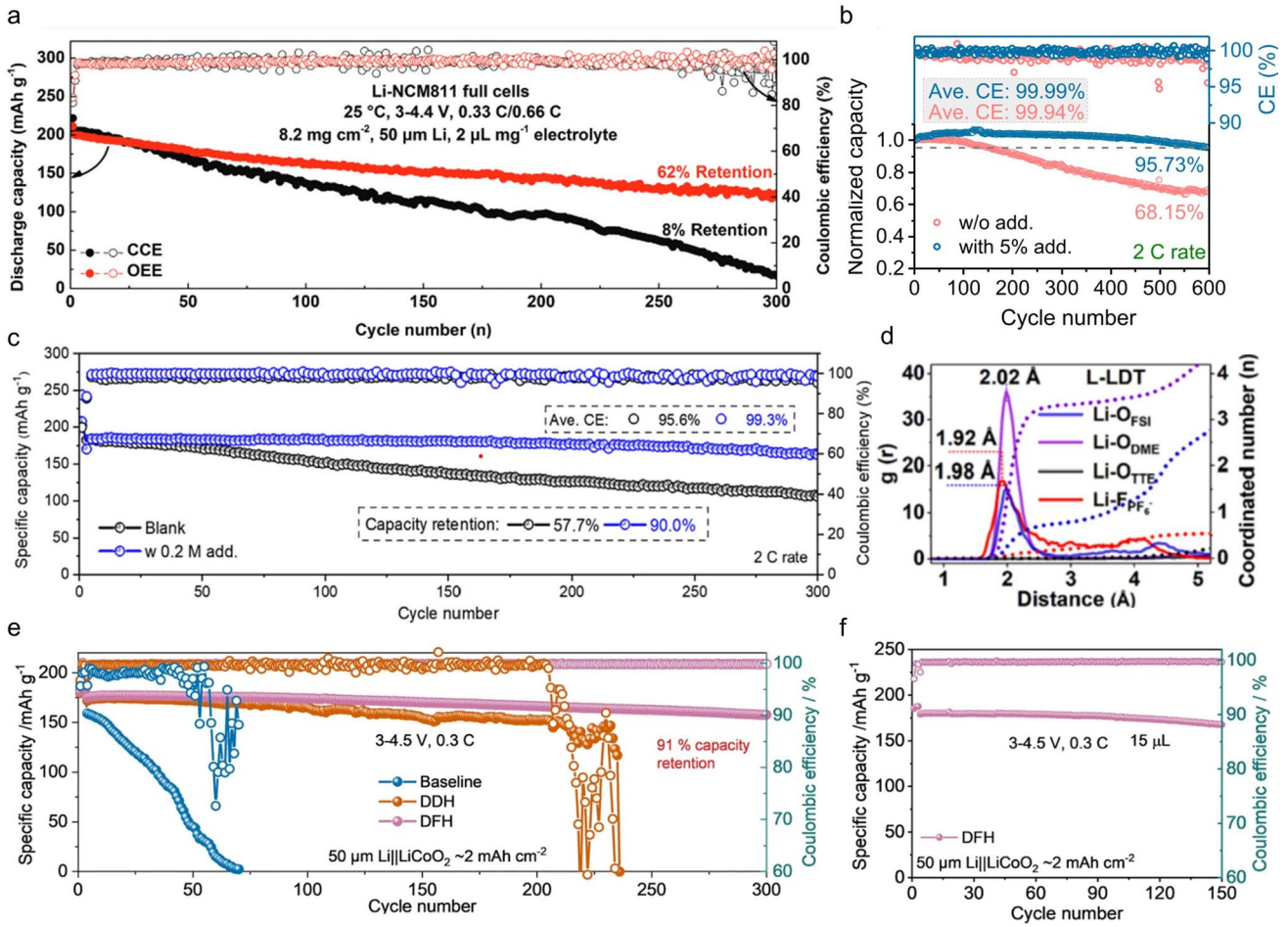

Fig. 6 **a** Comparison of cycling performance of Li-NCM811 full cell using different electrolytes at 25 °C (OEE:1 M LiDFOB in DME + 0.5 M $LiNO_3$ + 5 vt% VC; CCE: 1 M $LiPF_6$ in EC/DEC) [88]. Copyright 2023, Wiley–VCH GmbH. **b** Cycling performance and CE based on normalized capacity at the 2C rate in 1 M $LiPF_6$ in EC/DEC with and without $Cu(NO_3)_2$ additive [89]. Copyright 2021, American Chemical Society. **c** The electrochemical performance of Li|NCM811 cell with different electrolytes between 3.0 and 4.3 V at 2C rate [91]. Copyright 2022, Elsevier. **d** The corresponding RDF of the Li-O_{DME}, Li-O_{TTE}, Li-F_{PF6}, and Li-O_{FSI} pairs in 1.0 M LiFSI and 0.1 M $LiPF_6$ electrolytes in DME-hydrofluoroether (TTE) (with Li^+: DME = 1: 4) [92]. Copyright 2022, Elsevier. **e** Long-term cycling performance of Li||LCO cells using baseline, DDH, and DFH electrolytes. **f** Cycling performance of Li||LCO cells using DFH with limited conditions [20]. Copyright 2022, Springer Nature

 https://doi.org/10.1007/s40820-024-01629-5

strengthened. It is reasonable to infer that the enhanced interaction of Li^+-DME and the reduced number of free DME molecules will improve the high-voltage (4.3 V) stability of the L-LDT electrolyte.

Hee-Tak Kim has proposed a novel sulfur-containing species, thiocyanate (SCN^-), which exhibits both electron-donating and accepting properties for application in Li–S batteries [93]. The electron-deficient carbon atom provides high acceptor number (AN) functionality, while the electron-rich nitrogen and sulfur atoms provide high DN functionality. Molecular dynamics simulations and radial distribution functions show that high DN of SCN^- are more prone to participate in Li^+ solvation sheath, facilitating the formation of a Li_3N-rich AEI, thereby enhancing the reversibility of lithium metal anodes. Additionally, direct interaction between the high AN of SCN^- and polysulfides (PS) results in significantly high solubility of LiPS in LiSCN-based electrolytes, reinforcing the three-dimensional morphology of Li_2S by the solution-mediator. Li–S batteries employing this anion chemistry approach exhibit outstanding lithium metal stability.

Li et al. proposed that the electrostatic interaction between anions and solvents in the electrolytes (1 M LiDFOB in the mixture of 2,2,2-trifluoro-N, N-dimethylacetamide (FDMA) and 1,1,2,3,3,3-hexafluoropropyl-2,2,2-trifluoroethylether (HTE) (1: 1 by volume)) has an important impact on the solvation structures [20]. Based on the results of molecular dynamics calculations and characterization tests, it was found that interactions of appropriate strength between anion ($DFOB^-$) and solvent (FDMA) can promote more $DFOB^-$ to enter the solvation sheath, fostering the development of a stable SEI and exhibiting high Li^+ transport kinetics. Furthermore, benefiting from the fast ion transport kinetics through CEI film, excellent electrochemical performances for Li||LCO cell are achieved under the conditions of a high charge voltage of 4.5 V (Fig. 6e), the lean electrolyte of 15 µL (Fig. 6f), and a wide temperature range from − 20 to 60 °C.

LiF-rich SEI is usually a good strategy to improve interface issues. However, these fluorinated compounds (mainly $LiPF_6$) can lead to serious side effects (e.g., the production of the toxic gas HF) at high temperatures, causing irreversible damage to the battery. Li et al. successfully obtained a LMB with a stable LiF-free SEI by using a fluorine-free electrolyte (1 M LiBOB + 0.5 M $LiNO_3$ in DME) [94]. Specifically, when NO_3^- is introduced into the electrolyte, it preferentially enters the inner solvated sheath layer and participates in the decomposition to generate SEI, and the interface is characterized as a composite interface mainly rich in B/O/N, with excellent stability and fast lithium-ion transport capacity. As a result, the Li||LFP battery can achieve a very-fast-charging capability at 100C and 60 °C.

In addition to the high temperature, Kong et al. proposed weak–strong anions (FSI^-, NO_3^-) strategy to modulate the solvation sheath of lithium ions for achieving low-temperature LMBs [95]. The electrolyte based on weak FSI^- and the strong NO_3^- anion properly balances ion transport and the stability of aluminum surfaces, making NCM622||Li batteries can normally work for 120 cycles at − 20 °C with capacity retention of 80%.

3.2 Anion-Regulated Desolvation Process

As mentioned above, anions can regulate the solvation structure of Li-ion. Therefore, anions can regulate the desolvation process of Li-ion at the interface, which is very important for the charge transfer process. The coordinated solvents (anions), hydrogen bonds, and van der Waals forces can affect the desolvation process of Li-ion [80, 96–98]. Thus, the desolvation process can be understood as a decomposition coordination process with certain energy barriers [99]. That means the Li-ion will lose the coordinated solvents and anions through reorganization of the solvation structure. The process involves charge transfer, which is critical to the dynamics of the battery.

Anion regulation is a good optimization method to mediate the desolvation process of Li-ion. Li et al. used TFA^- to adjust the solvation sheath environment of Li^+ and promote fast desolvation dynamics due to its high DN (34.0 kcal mol^{-1}) [36]. By comparing the LUMO of various substances (Fig. 7a), it is evident that TFA^- is more prone to decomposition, preferentially forming a stable SEI rich in LiF and Li_2O. E_{a2} represents the energy barrier of Li^+ desolvation from the Li^+ solvation sheath. Compared with the E_{a2} in $LiPF_6$-EC/ DEC (69.14 kJ mol^{-1}) and $LiPF_6$-DME/ FEC (64.92 kJ mol^{-1}), the energy of LiTFA-DME/FEC (60.02 kJ mol^{-1}) showed a slight decrease (Fig. 7b). The decreased energy barrier proves that TFA^- in the Li^+ solvation sheath has a significant effect on the Li^+ transport kinetics of SEI. Li et al. designed a dual-salt (0.5 M LiTFA, 0.5 M LiTFSI)-based electrolyte with G4 (tetraethylene

glycol dimethyl ether) as the solvent in $Li-O_2$ batteries [100]. This electrolyte slows down the decomposition of G4 and induces a SEI rich in inorganic substances. Electrostatic potential (ESP) calculations showed that the smaller volume of TFA^- is more concentrated in negative charge compared to $TFSI^-$. As a result, Li^+ is more readily attracted to the TFA^-, thus reducing the binding strength to the G4. Further studies calculated the binding energies of G4 molecules to Li^+ within solvated configurations containing different anionic coordination. As the number of TFA^- rises, the G4 binding energy decreases, suggesting that the enhanced anionic coordination induces a decrease in the Li^+-solvent binding strength. The mean square displacement (MSD) suggests that the Li^+ mobility is enhanced due to the weakened binding by G4 molecules. Meanwhile, compared with 1.0 M LiTFSI in G4, the TFA^- helps to reduce the energy barrier for desolvation (Fig. 7c). They also introduced TFA^- into G2-based (Bis(2-methoxyethyl)ether) electrolytes, enabling the regulation of solvation chemistry under low-temperature conditions to achieve highly stable SIB_s [101]. Compared with 1.0 M $NaPF_6$ in G2, TFA^- anions gradually occupy the majority of the solvated structure, while the G2 molecules are squeezed out. The unique solvation structure accelerates the desolvation of Na^+ by decreasing the desolvation energy

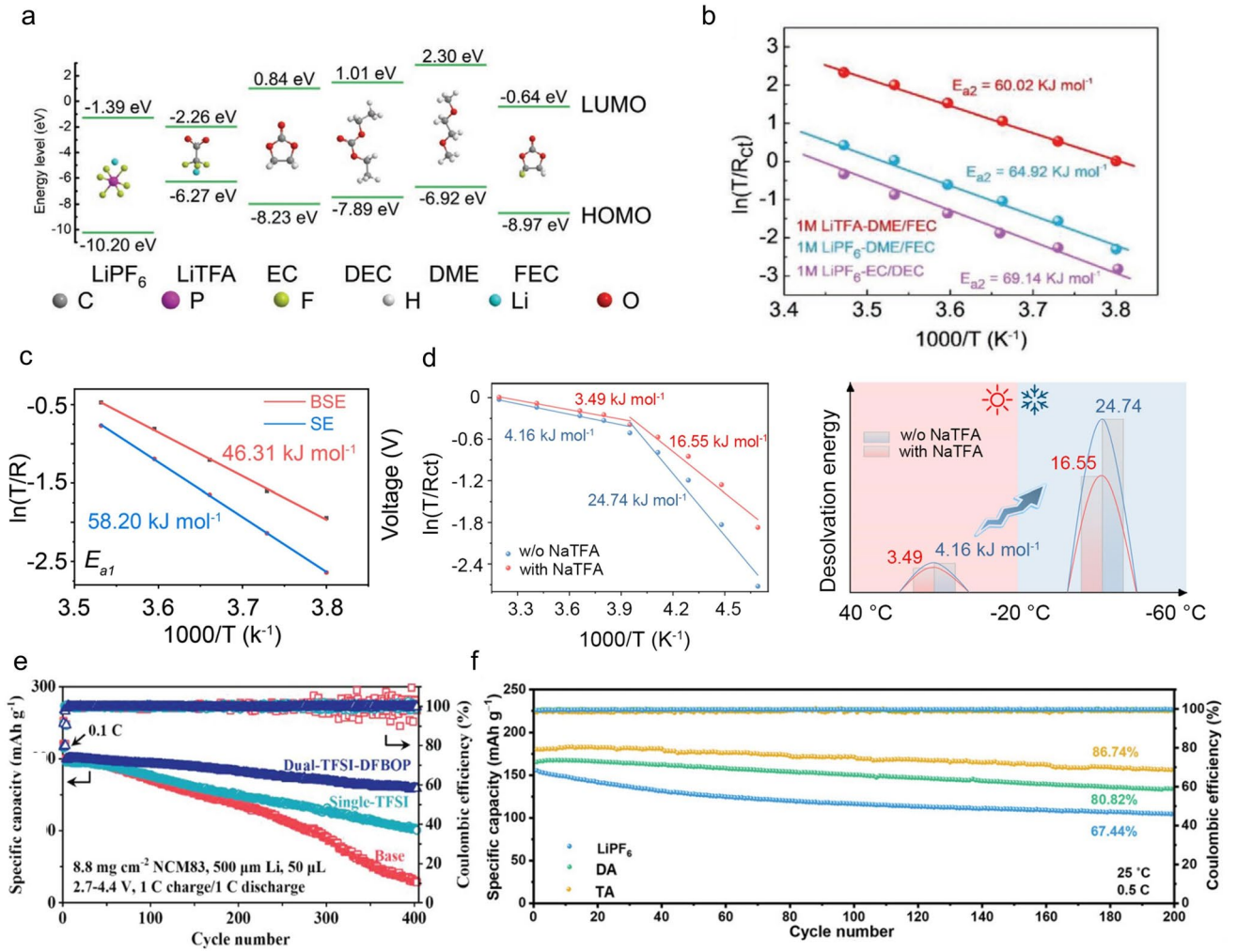

Fig. 7 **a** Molecular orbital energy of different anions and solvents. **b** Activation energies derived from Nyquist plots [36]. Copyright 2020, Wiley-VCH Verlag. **c** Activation energies of Li^+ desolvation (E_{a1}) in SE and BSE electrolyte [100]. Copyright 2023, Wiley–VCH GmbH. **d** Desolvation energy of Na^+ derived from Nyquist plots and Schematic of desolvation energy in a wide temperature range [101]. Copyright 2024, National Academy of Sciences. **e** Electrochemical performance of Li||NMC83 coin cells in different electrolytes[102]. Copyright 2023, Wiley–VCH GmbH. **f** Cycling performance of Li||NCM811 cells using $LiPF_6$, DA, and TA electrolytes at 0.5C and 25 °C [103]. Copyright 2024, Wiley–VCH GmbH

https://doi.org/10.1007/s40820-024-01629-5

from 4.16 to 3.49 kJ mol^{-1} and 24.74 to 16.55 kJ mol^{-1} at 40 to − 20 °C, respectively, compared with that in 1.0 M $NaPF_6$-G2 (Fig. 7d).

Xu et al. developed a dual-anion modulator strategy for designing a good electrolyte for LMBs [102]. The $TFSI^-$ anion can regulate the solvation structure of Li^+ to produce a low Li^+ desolvation energy, while $DFBOP^-$ promotes the formation of high ion conductivity and sustainable inorganic-rich SEI on both sides. Impressive cycling performance of the cell was achieved in a dual-TFSI-DFBOP electrolyte, with high capacity retention of 80.5% after 400 cycles and a high CE of 99.9%. In contrast, the Li||L $iNi_{0.83}Co_{0.11}Mn_{0.06}O_2$ batteries showed a fast capacity fading, with only 14.4% and 51.5% capacity retention in base (1 M $LiPF_6$ in FEC/EMC) and single-TFSI electrolyte, respectively (Fig. 7e). Moreover, Cheng et al. designed a ternary salts-based electrolyte ($LiNO_3$, $LiPF_6$, and LiTFSI in THF-FEC solvent), which exhibits reduced Li^+ desolvation energy, making rapid charge transfer kinetics and a cold-resistant electrolyte [103]. Specifically, the strong interaction between NO_3^- and Li^+ weakens the interaction between PF_6^-/$TFSI^-$ anions and Li^+. In order to further investigate the binding energy of Li^+ with one or more anions, DFT calculations were performed. It was found that Li^+ had the lowest binding energy (− 4.62 eV) with the ternary anions. The optimized electrolyte demonstrates a high ionic conductivity of 3.39 mS cm^{-1} at − 60 °C and good compatibility with the lithium metal anode. Additionally, the lithium metal anode is effectively shielded from dendrite growth by a sturdy AEI derived from the anions. Moreover, the NCM811 cathode experiences reduced particle cracking due to a robust CEI. As shown in Fig. 7f, the ternary salts electrolyte enables Li||NCM811 cell to cycle stably at room temperature (25 °C) with a specific discharge capacity of 180.3 mAh g^{-1} and capacity retention of 86.74% after 200 cycles at 0.5C.

3.3 Antioxidant Properties Affected by the Anion-Modulated Solvation

The developing of high-voltage batteries has faced challenges such as designing a suitable electrolyte, especially for the LMBs. Ether electrolytes are considered suitable for LMBs due to their compatibility with lithium metal. However, they cannot endure high voltages. Researchers usually apply high-concentrated electrolytes (HCE) [104, 105] or localized high-concentrated electrolytes (LHCE) [11, 106] strategies to improve the compatibility of both sides. Currently, the weakly solvating electrolytes (WSE) [107, 108] are confirmed an effective strategy to modify the electrochemical performance. The HCE strategy increases lithium salt concentration to reduce free solvents (increase the ratio of salt/solvent, Fig. 8a), constructing an anion-rich solvation structure which helps form a stable SEI. However, the high viscosity, low ionic conductivity, and high cost of HCEs limit their practical use. LHCE strategy mitigates these issues by using inert diluents (weak solvent), which can also maintain the anion-rich solvation structure. WSE strategy applies low-solvating-power solvents to encourage ion pairing, enhancing SEI stability but potentially reducing ionic conductivity. It should be noted that the above-mentioned strategies can be achieved by regulating the solvent (solvent chemistry). In comparison, anions can play a prominent role in electrolyte design (anion chemistry, Fig. 8a). By optimizing the structure and properties of anions, the solvation structure can be directly controlled. Unlike traditional methods, the anion chemistry is a new strategy to regulate the solvation structure, enabling the electrolyte good electrochemical performance like high-voltage stability.

Our group proposed a new strategy to tune the solvation structure of Li-ion by anion chemistry [35]. We utilized the high DN of NO_3^- to coordinate with Li^+, competing with DME in the solvation process. The NO_3^- weakens the solvating ability of DME, and this competition reduces the number of solvated molecules, thereby lowering the likelihood of solvent oxidation at high potentials. As a result, an anion-regulated weakly solvating electrolyte (ARWSE) is formed (Fig. 8a). Even at a high voltage of 4.5 V, the electrolytes with NO_3^- can normally work (Fig. 8b). Additionally, characterization experiments have confirmed that ARWSE promotes the formation of inorganic-rich components in the AEI/CEI, effectively suppressing continuous electrolyte decomposition and aluminum corrosion, thereby improving the antioxidant performance and coulombic efficiency of the battery. Li et al. achieved stable LMBs with DME electrolyte at 4.6 V (Fig. 8c), regulated by BF_4^- anion [109]. The strong electrostatic attraction between Li^+ and BF_4^- causes more anions to be distributed in the first solvation shell, preferring to generate inorganic-rich SEI/CEI. Benefiting from its unique solvation structure, the oxidation resistance of the electrolyte is greatly increased (from 4.3 to 4.6 V). Guo et al. designed a THF-based electrolyte using

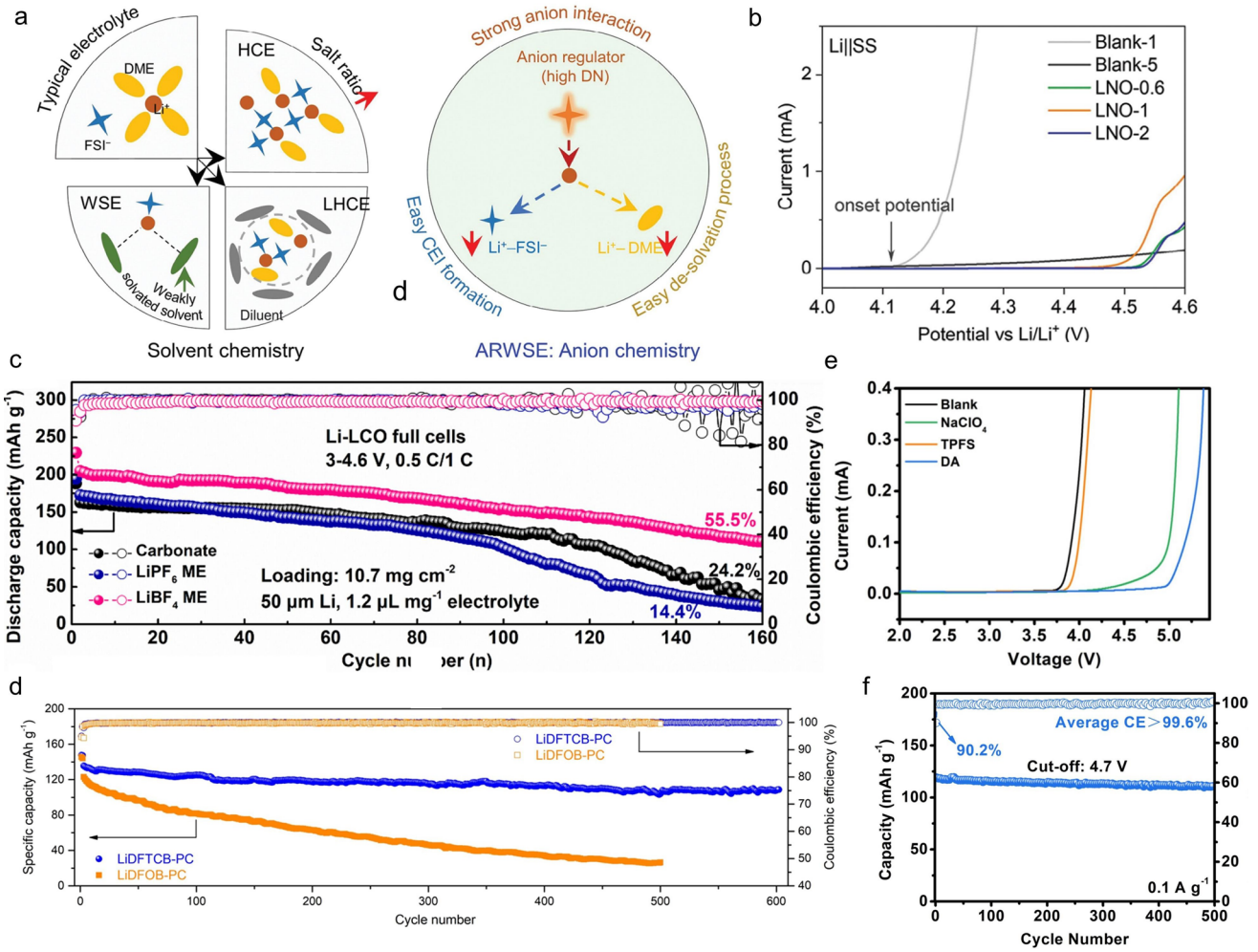

Fig. 8 **a** Comparison between typical solvent chemistry and anion chemistry. **b** LSV profiles of Li||SS cells at a scan speed of 0.1 mV s^{-1} in different electrolytes[35]. Copyright 2023, Wiley–VCH GmbH. **c** Cycling performance of Li||LCO full cells with various electrolytes [109]. Copyright 2023, Wiley–VCH GmbH. **d** Cycling performance of the LCO||graphite full cells using LiDFTCB-PC and LiDFOB-PC electrolyte at room temperature [111]. Copyright 2023, Wiley–VCH GmbH. **e** LSV test of various electrolytes at a scanning rate of 2 mV s^{-1}. **f** Cycling performance of Na||NVPF in 1 M $NaPF_6$ in a mixed solvent of EC and DEC (1:1 by volume ratio) with trimethoxy(pentafluorophenyl)silane (TPFS) and $NaClO_4$ [112]. Copyright 2022, Wiley–VCH GmbH

dual salts of LiTFSI and $LiNO_3$ [110]. They confirmed the interaction between the anion and the solvent, finding that the $TFSI^-$ anion further enhanced the interaction between NO_3^- and THF, and the reduction in the number of free THF molecules favored the enhancement of the oxidative stability of the electrolyte. The SiO_x||NCM811 full cell using the designed ether-based electrolyte can still maintain 81.7% of the initial capacity after 500 cycles at 4.3 V, which is higher than that in the EC-based electrolyte (34.7%).

Cui and colleagues successfully synthesized a cyanide-containing lithium salt: lithium difluoro(1,2-dihydroxyethane-1,1,2,2-tetracarbonitrile) borate (LiDFTCB) [111]. They found that using LiDFTCB/PC electrolyte, the graphite||LCO full cell demonstrates high capacity retention of 80.2% after 600 cycles at 25 °C and 0.5C. In sharp contrast, LiDFOB-PC shows poor electrochemical compatibility with the graphite||LCO cell, delivering a dramatically low-capacity retention of 21.5% (Fig. 8d). The HOMO energy level of $DFTCB^-$ is lower than that of $DFOB^-$, indicating higher oxidative stability of $DFTCB^-$. Additionally, electrochemical characterization revealed that the oxidation stability of the LiDFTCB-based electrolyte is superior to that of the LiDFOB-based electrolyte, ascribing to the replacement of the –C=O

 https://doi.org/10.1007/s40820-024-01629-5

moieties by four – C≡N groups. Results reveal that more $DFTCB^-$ anions and less PC solvent are involved in the solvation structure of Li^+. The high coordination number of $DFTCB^-$ with Li^+ will lower the LUMO energy level of the anion, which favors the formation of inorganic-rich SEIs on the anode. This prevents severe capacity degradation of the battery at 50 °C. In comparison, LiDFOB undergoes severe decomposition at 50 °C. While using LiDFTCB salt, no CO_2 gas was detected at 50 °C.

In addition to the application of anion-regulation for lithium batteries, Ma et al. stabilized a electrolyte (1 M $NaPF_6$ in EC/DEC) for 4.7 V SIBs by rationally configuring the solvated structure of the electrolyte with $NaClO_4$ and trimethoxy(pentafluorophenyl)silane (TPFS) as dual additives (Fig. 8e, f) [112]. Here ClO_4^- as the voltage-stimulated response species tends to rapidly move to the cathode surface during the charging process, then binds with Na^+ and solvents to form polymer-like structures (ClO_4^--Na^+-solvent), which dramatically reduces the continuous solvent decomposition at high voltages. Meanwhile, the Si – O derived from TPFS can effectively capture adverse species such as HF and H_2O, generating Si – F and Si – O, which could well protect CEI integrality and suppress CEI dissolution. Thus, these two additives increase the oxidative stability of the carbonate electrolyte from 3.77 to 4.75 V. Na||$Na_3V_2(PO_4)_2O_2F$ cells using the optimized electrolyte achieve a stable cycling performance at 4.7 V, with 93% capacity retention after 500 cycles and 99.6% average CE.

4 Flame-Retardant Applications by Halogen Anions

In addition to the requirement of high energy density for a battery, the safety issue is also very important. Halogen-containing flame retardants can be divided into fluoride, chloride, and bromide-containing flame retardants. When subjected to heat, the halogen can produce free radicals, inhibiting the combustion process [113]. At present, F-, Cl-, and Br-type flame-retardant additives are widely used, while I-type flame-retardant additives are less used. This is because the C-I bond is too weak to remain stable [114]. Among the halogen-containing flame retardants for LIBs, F-substituted compounds are the most studied. Fluorinated compounds can increase the flash point of the electrolyte, reduce the flammability of the electrolyte, and promote the generation of SEI film on the anode surface to improve the performance of the battery [115–118].

The introduction of fluorine atoms into the ester solvents results in a lower LUMO (Fig. 9a, b), which can be preferentially reduced on the lithium metal surface, resulting in the formation of a LiF-rich solid electrolyte interface, which inhibits the growth of lithium dendrites [119]. Therefore, the optimized electrolyte (1 M $LiPF_6$ in FEC BTC) used in Li||NCM811 batteries can operate within a wide operating temperature range of – 30 to 70 °C. More importantly, during flame-retardancy tests, the optimized electrolyte is non-flammable (Fig. 9c), implying its stability at high temperatures and safety in practical use. Similarly, researchers also introduced fluorine atoms into ether solvents and found that fluorine atoms not only improve the flame-retardant properties of the solvent but also enhance the oxidation stability of the electrolytes [120]. Compared with the C-F bond (115 kcal mol^{-1}), the C–Cl bond (83.7 kcal mol^{-1}) is more prone to break, with the production of chloride radicals, which can effectively capture the highly active H· and generate HCl. The generated HCl can also capture ·OH and generate Cl· which can re-participate in the above reaction to effectively suppress the progress of combustion. As shown in Fig. 9d, the Cl-DEE (1,2-bis(2-chloroethoxy)-ethyl ether) has a lowered HOMO than the DEE, indicating improved oxidation stability. Moreover, the flash point of Cl-DEE is 126 °C, which is much higher than the 35 °C of DEE. The electrolyte (LiFSI in Cl-DEE/TTE, 1:1.6:3 by molar) provides excellent electrochemical stability even under ultra-high-voltage conditions (4.6 V).

Solid electrolytes offer a higher level of safety compared to liquid electrolytes [121–123]. Huang et al. designed a novel solid-state polymer electrolytes (SPEs) based on nonflammable polyurethane, which is covalently bound with reactive brominated flame retardant on the backbone [39]. Brominated flame retardants can participate in the formation of LiBr-rich SEI, which can enhance the stability of the electrolytes. Furthermore, the prepared polymer electrolytes have good electrochemical properties. The Li||SPEs||Li symmetric battery can undergo stable cycling for more than 2100 h. The Li||SPEs||$LiNi_{0.6}Co_{0.2}Mn_{0.2}O_2$ battery maintains capacity retention of 85.2% after 330 cycles at 0.3C. In contrast, the cell with unimproved electrolytes showed a reversible specific capacity of

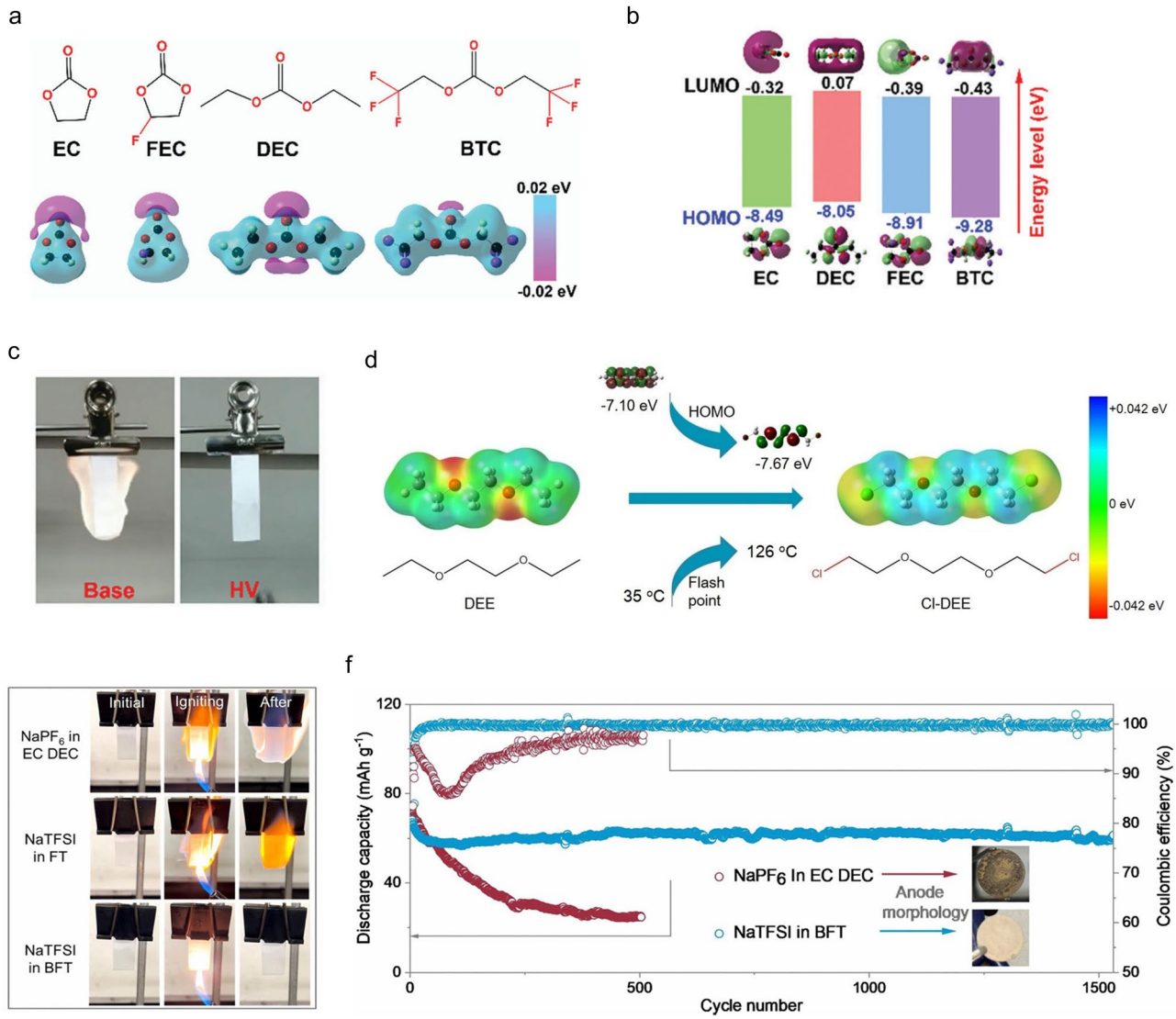

Fig. 9 **a** Molecular structure of various solvents and their corresponding charge distributions. **b** Molecular orbital energies of different solvents. **c** Flammability tests of the HV electrolyte composed of 1 M $LiPF_6$ in a mixture of FEC and bis(2,2,2-trifluoroethyl) carbonate (BTC) and base electrolyte:1 M $LiPF_6$ in a mixture of EC and DEC [119]. Copyright 2022, The Royal Society of Chemistry. **d** Design scheme and molecular structures of DEE and Cl-DEE [120]. Copyright 2022, Wiley–VCH GmbH. **e** Ignition experiments of $NaPF_6$ in EC/DEC, NaTFSI in FT and NaTFSI in BFT electrolytes. **f** Cycling performance of $Na_3V_2(PO_4)_3$||Na cells in different electrolytes at 300 mA g^{-1} [124]. Copyright 2024, Royal Society of Chemistry

162 mAh g^{-1} during the activation cycles and then decayed to 68 mAh g^{-1} after 200 cycles.

There is a wide variety of brominated compounds with excellent flame-retardant effects and wide applications, but relatively few studies have been conducted in LIBs. Researchers have developed a novel brominated flame-retardant 2-bromo-1-(2-bromoethoxy) ethane (BBE) solvent to improve the flame-retardant efficiency of SIBs [124]. Moreover, due to the low energy barrier for the dissociation of free radical scavengers, the Br-based flame retardants show the best response compared with the F-based, Cl-based, and P-based flame retardants (Fig. 9e). Br-based solvents lead to the formation of NaBr-rich SEI on the sodium metal. Due to its high ion conductivity, it inhibits the growth of sodium dendrites. Additionally, the Na||$Na_3V_2(PO_4)_3$ battery exhibits excellent cycling performance with a high capacity retention of 91.3% after 1500 cycles (Fig. 9f). In contrast, the capacity retention of cells

 https://doi.org/10.1007/s40820-024-01629-5

utilizing $NaPF_6$ in EC/DEC decreased to 80% after only 60 cycles.

5 Other Effects of Anions

In addition to what we mentioned above, there are also other effects influenced by anions. Huang et al. reported that ClO_4^- can change the decomposition path of $TFSI^-$ as catalysis, enabling the complete decomposition of $TFSI^-$, thereby forming an excellent SEI [125]. Specifically, high-resolution spectra of F 1*s* (Fig. 10a) clearly showed higher intensity of LiF in SEI after adding $LiClO_4$, further unambiguously confirming that the association generated by $LiClO_4$ contributes to the decomposition reaction of LiTFSI. A similar phenomenon was also found for high-resolution spectra of S 2*p* (Fig. 10b). The relative content of S atoms was at a low level without adding $LiClO_4$, represented by the weak peak intensity of the reduction products. With increasing the content of $LiClO_4$, the content of RSO_3Li, Li_2S, Li_2S_x, and Li_2SO_3 increased significantly. As a result, the use of $LiClO_4$ effectively improves the CE and cycle life of the LMBs.

Xie et al. observed that LiDFOB can change the traditional decomposition path of ether solvents, thereby improving the high-voltage stability of the electrolytes (Fig. 10c) [126]. It is found from the calculation that LiDFOB can preferentially catalyze DME to generate LiF and lithium mono(oxalate) borate (LiMOB). LiMOB can further trigger the polymerization reaction of DME to generate polyMOBs, thereby inhibiting the continuous decomposition of DME at the positive electrode. A thin and uniform organic–inorganic composite CEI was formed on the surface of LCO with the LiDFOB salt. This unique structure can effectively protect the LCO cathode and inhibit adverse reactions at the positive electrode. In addition, new chemical bonds and functional groups can be identified by Fourier transform infrared spectroscopy (FTIR) after the electrolyte decomposition, further supporting the pathway switching mechanism that altered the degradation process of

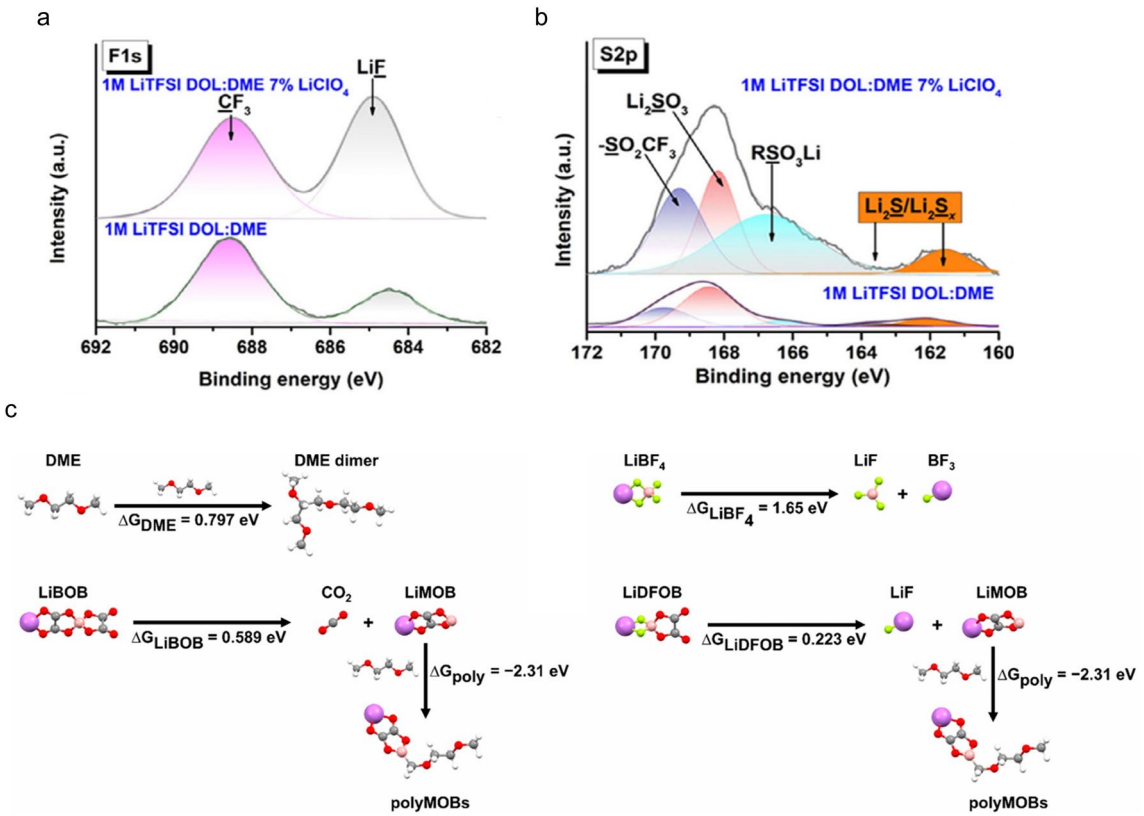

Fig. 10 XPS spectra of the formed SEI in different electrolytes for **a** F 1*s* and **b** S 2*p* before and after the adding of $LiClO_4$ [125]. Copyright 2019, Published by Elsevier. **c** Optimized geometries and the corresponding decomposition reaction free energies of DME, $LiBF_4$, LiBOB, and LiDFOB at high-voltage [126]. Copyright 2023, American Chemical Society

the DME. Zhao et al. also reported that a small amount of LiDFOB additive can alter the decomposition pathway of trans-difluoroethylene carbonate (DFEC) [127]. The presence of LiDFOB can significantly induce the direct defluorination of DFEC, accompanied by the formation of inorganic species such as LiF and Li_xBF_y. The defluorinated DFEC with high reactivity can polymerize into highly elastic poly (VC), which will interweave with the concurrently generated LiF, forming a distinctive SEI with a LiF-dominated inner layer and a LiF-polymeric interwoven outer layer. This SEI film exhibits excellent mechanical stability and good ion transport properties, significantly improving the cycling and rate performance of the silicon anode.

Anion chemistry is also widely used in dual-ion battery [128, 129]. For example, Cui et al. designed an anion-permselective polymer electrolyte that preferentially coordinates PF_6^- with a quaternary ammonium group, enhancing PF_6^- desolvation and improving the structural integrity of graphite electrodes while increasing electrolyte oxidative stability [130]. Tang et al. developed a high-concentration LiFSI electrolyte, which promotes the formation of a stable SEI layer, enhancing the full-cell energy density by suppressing gas formation at high voltages [131].

6 Summary Outlook

We have emphasized the roles of different anions in the electrolyte and summarized the effects of anions on surface interfacial chemistry, solvation structure, and electrochemical stability. Although the anion chemistry in electrolytes is still in its early stages of research, it has made significant progress in energy storage, safety issues, interfacial chemistry, and kinetics. This research direction is increasingly gaining attention and will undoubtedly guide research efforts in the field of energy storage. For specific battery systems, significant stability improvements can be achieved by selecting suitable anion(s). Here we give a summary of the characteristics of the mentioned anions, which is also shown in Table 1. It should be noted that DN is selected as a representative parameter to describe the coordination ability of the anions and solvents with Li-ions, helping to infer the solvation structure which directly connected with SEI formation. However, parameters such as LUMO, HOMO, activation energy, and binding energy also play a role in selecting anions and solvents. A more accurate choice may be made with the help of DFT calculations.

The FSI^- anion and the $TFSI^-$ anion play crucial roles in protecting the negative electrode, forming a stable SEI, and enhancing ion transport performance. The FSI^- anion exhibits good electrochemical stability at low temperatures, making it suitable for wide temperature range applications. While the $TFSI^-$ exhibits resistance to hydrolysis and possesses high ion conductivity and commendable thermal stability. However, electrolytes based on FSI^- and $TFSI^-$ cannot effectively passivate aluminum foil current collectors, especially at high operating voltages.

Nitrate anions in batteries have several advantages such as forming a protective film on the electrode surface. They possess good adsorption properties, helping to regulate the chemical properties of the electrode interface. They can also adjust the solvation structure of solvent molecules in the electrolyte, optimizing ion transport performance. NO_3^- complex with Al^{3+} on the surface of aluminum foil forms a passive layer containing AlN, inhibiting the corrosion of aluminum. Additionally, nitrate anions are inexpensive, and price-friendly. However, nitrate anions have low solubility in ester solvents, limiting their application in certain electrolyte systems. Furthermore, as sacrificial additives, nitrate anions are gradually consumed during battery reactions and need periodic replenishment, which affects the long-term usage of the battery.

PF_6^- anion can form a stable protective layer on an aluminum current collector, effectively preventing aluminum corrosion and significantly extending battery lifespan. Additionally, during battery operation, PF_6^- anion decomposes to form a conductive SEI enriched with LiF. This interface layer not only enhances the stability of the cathode but also improves battery performance. However, shortcomings such as poor hydrolytic stability, insufficient thermal stability, and sensitivity to moisture limit their application in more demanding or extreme environments.

LiDFOB forms a new structure within the IHP, facilitating the formation of a robust CEI, thereby preventing the dissolution of the active material. This interface layer effectively prevents adverse reactions between electrolyte components and solvents, significantly extending battery life and enhancing electrolyte stability. Additionally, LiDFOB can alter the decomposition pathway of some solvents, enhancing battery stability at high voltages and further improving battery performance.

 https://doi.org/10.1007/s40820-024-01629-5

Table 1 The role of different anions and their limitations. (The structures of these anions are shown in Fig. 1) Here n/a means not applicable

Anion	Primary Roles	Limitations
FSI^-	Stable SEI; wide temperature range stability; high ion transport; SEI repair agent	Aluminum corrosion at high voltages
$TFSI^-$	Hydrolysis resistance; stable SEI; high ionic conductivity; thermal stability	Aluminum corrosion at high voltages
NO_3^-	N-rich SEI; solvation structure regulator; adsorbent	Low solubility in ester solvents; sacrificial agent
PF_6^-	Stable CEI; aluminum current collector protection	Poor hydrolytic and thermal stability; sensitive to moisture
$DFOB^-$	Stable CEI; alters solvent decomposition pathways; high voltage stability	Low solubility; produces harmful gases at high temperatures
ClO_4^-	Stable CEI; synergistic film formation	Strong oxidizing properties; risk of side reactions at high voltages
FFF^- & FBF^-	Stable SEI (LiF/LiBr-based SEI); good cathodic degradability; high Li^+ selectivity	n/a
FEA^-	SEI repair agent; dissolves organic impurities; high molecular dipole; high DN; high t_{Li+}	Excessive SEI dissolution; nucleophilic reactivity
$ETFSI^-$	SEI repair agent; dissolves organic impurities	n/a
SCN^-	Stable SEI; high oxidation resistance	Poor conductivity
CN^-	Synergistic film formation; removes water and acid	Strong oxidizing properties
TFA^-	Solvation sheath regulator; rapid ion transport; enhances oxidation resistance	Lower dissociation degree; lower overall conductivity
$DFBOP^-$	Inorganic-rich SEI; high ionic conductivity	n/a
BF_4^-	Good oxidative stability; robust SEI; high temperature stability; corrosion resistance	Limited ionic conductivity; low solubility
I^-/I_3^-	Repairs agent of dead lithium; improves fast-charging stability in lithium metal batteries	n/a
F-, Cl-, Br-, I-based flame retardants	Flame retardancy; stable SEI; enhances high-temperature safety	Iodine-based compounds are less stable

The role of ClO_4^- in batteries enhances performance by optimizing the formation and stability of the CEI and promoting Li^+ transport. Moreover, it has the role of a catalyst when coupled with some anions/solvents, making a good SEI formation to prevent lithium dendrite growth and extend battery life. However, electrolytes containing ClO_4^- have strong oxidizing properties, which can easily trigger side reactions at higher voltages, causing battery swelling and posing safety issues.

LiFFF and LiFBF are more easily electrochemically reduced on the anode surface and form LiF/LiBr-rich SEIs to passivate the lithium metal anode. LiFEA dissolves organic impurities and promotes the enrichment of inorganic substances, optimizing and stabilizing the SEI layer. In addition, another salt, LiETFSI, is superior to LiFEA in dissolving oxygenated organic compounds in the SEI while reducing the dissolution of inorganic components such as LiF. The SCN^-, as an electrolyte additive in LMB, significantly enhances the performance and stability of lithium metal anodes by its solvation properties and the formation of a stable SEI. The CN^- in LMB primarily functions to inhibit the dissolution of Co ions. It achieves this by forming a dual-layer CEI consisting of an inner LiF layer and an outer layer rich in $B-F/-CN$ organic structures. These actions collectively enhance the stability and performance of the battery.

The high DN of TFA^- regulates the solvation sheath environment of Li^+ and promotes rapid dissolution kinetics. The main role of $DFBOP^-$ in sodium-ion batteries is to preferentially decomposition on both the positive electrode and metal negative electrode sides, forming stable and robust CEI/AEI. These interfaces contain inorganic substances, significantly enhancing the stability. The strong electrostatic attraction between Li^+ and BF_4^- leads to more anions distributed in the first solvated shell layer, which greatly reduces the number of free anions. Due to its unique solvated structure, the oxidation resistance of the cell is greatly enhanced.

The use of a reversible I^-/I_3^- redox reaction can deal with the deposition of dead lithium on the anode, which is an

effective strategy to improve the performance of LMB even under fast-charging conditions. Moreover, halogen-containing flame retardants play a critical role in enhancing the safety and performance of battery electrolytes. By capturing free radicals and forming stable SEI, these compounds mitigate the risks associated with high temperatures and dendrite formation, while also significantly improving the overall electrochemical stability of the batteries.

In summary, the anions' involvement in the solvation structure can greatly influence the electrochemical stability of the electrolyte. However, characterization methods are not yet sufficient and mature enough to obtain accurate solvation structure and dynamic information, especially during battery cycling. It is also important to elucidate the formation and composition of the interfacial film generated by anions and solvents. The design of a uniform and stable SEI is crucial for enhancing the electrochemical stability of the electrolyte and stabilizing both negative and positive electrode materials. This requires a comprehensive understanding of the thermodynamics and kinetics of anion decomposition. Furthermore, studying the plating/stripping behavior of metal anodes (Li^0, Na^0) is crucial for improving the cycle stability of metal batteries. Analyzing the role of anions in these processes is an effective strategy to achieve the goal, sometimes the combination of the multiple anions is better. In the future, there will be further exploration of novel anion chemistry. Through the structural design of the anions, it will be possible to precisely control the anion chemistry to enhance energy density, cycle life, and safety of the batteries. At the same time, by integrating the popular artificial intelligence computing technologies, it is possible to better predict and optimize the performance of electrolytes, driving innovation and development in this field. In conclusion, the future development of the electrolyte field can be achieved not only through the design, development, and application of anions but also through the development of new solvents, laying a solid foundation for the next generation of high-performance and safe battery technologies.

Acknowledgements This work was supported by National Key Research and Development Program of China (2022YFB2402200), the China Postdoctoral Science Foundation (grant nos. 2023T160591), and the Joint Fund of the Technical R&D Program of Henan Province (grant nos. 232301420044).

Authors' Contributions Hecong Xiao did investigation and original draft writing. Xiang Li & Yongzhu Fu supervised and done review and editing.

Declarations

Conflict of Interest The authors declare no interest conflict. They have no known competing financial interests or personal relationships that could have appeared to influence the work reported in this paper. Dr. Hao Tian is an assistant editor for Nano-Micro Letters and was not involved in the editorial review or the decision to publish this article. All authors declare that there are no competing interests.

References

1. J. Xu, J. Zhang, T.P. Pollard, Q. Li, S. Tan et al., Electrolyte design for Li-ion batteries under extreme operating conditions. Nature **614**, 694–700 (2023). https://doi.org/10.1038/s41586-022-05627-8
2. A.-M. Li, O. Borodin, T.P. Pollard, W. Zhang, N. Zhang et al., Methylation enables the use of fluorine-free ether electrolytes in high-voltage lithium metal batteries. Nat. Chem. **16**, 922–929 (2024). https://doi.org/10.1038/s41557-024-01497-x
3. Q. Li, C.-G. Han, S. Wang, C.-C. Ye, X. Zhang et al., Anionic entanglement-induced giant thermopower in ionic thermoelectric material Gelatin-CF_3SO_3K–CH_3SO_3K. eScience **3**, 100169 (2023). https://doi.org/10.1016/j.esci.2023.100169
4. X. Fan, C. Wang, High-voltage liquid electrolytes for Li batteries: progress and perspectives. Chem. Soc. Rev. **50**, 10486–10566 (2021). https://doi.org/10.1039/d1cs00450f
5. Y. Qiao, H. Yang, Z. Chang, H. Deng, X. Li et al., A high-energy-density and long-life initial-anode-free lithium battery enabled by a Li_2O sacrificial agent. Nat. Energy **6**, 653–662 (2021). https://doi.org/10.1038/s41560-021-00839-0
6. Y. Yamada, J. Wang, S. Ko, E. Watanabe, A. Yamada, Advances and issues in developing salt-concentrated battery electrolytes. Nat. Energy **4**, 269–280 (2019). https://doi.org/10.1038/s41560-019-0336-z
7. J. Alvarado, M.A. Schroeder, T.P. Pollard, X. Wang, J.Z. Lee et al., Bisalt ether electrolytes: a pathway towards lithium metal batteries with Ni-rich cathodes. Energy Environ. Sci. **12**, 780–794 (2019). https://doi.org/10.1039/C8EE02601G
8. X. Ren, L. Zou, S. Jiao, D. Mei, M.H. Engelhard et al., High-concentration ether electrolytes for stable high-voltage

lithium metal batteries. ACS Energy Lett. **4**, 896–902 (2019). https://doi.org/10.1021/acsenergylett.9b00381

9. C. Tian, K. Qin, L. Suo, Concentrated electrolytes for rechargeable lithium metal batteries. Mater. Futur. **2**, 012101 (2023). https://doi.org/10.1088/2752-5724/acac68
10. S. Lin, H. Hua, P. Lai, J. Zhao, A multifunctional dual-salt localized high-concentration electrolyte for fast dynamic high-voltage lithium battery in wide temperature range. Adv. Energy Mater. **11**, 2101775 (2021). https://doi.org/10.1002/aenm.202101775
11. S. Chen, J. Zheng, D. Mei, K.S. Han, M.H. Engelhard et al., High-voltage lithium-metal batteries enabled by localized high-concentration electrolytes. Adv. Mater. **30**, 1706102 (2018). https://doi.org/10.1002/adma.201706102
12. T.D. Pham, A. Bin Faheem, J. Kim, H.M. Oh, K.K. Lee, Practical high-voltage lithium metal batteries enabled by tuning the solvation structure in weakly solvating electrolyte. Small **18**, e2107492 (2022). https://doi.org/10.1002/smll.202107492
13. T.D. Pham, K.K. Lee, Simultaneous stabilization of the solid/cathode electrolyte interface in lithium metal batteries by a new weakly solvating electrolyte. Small **17**, e2100133 (2021). https://doi.org/10.1002/smll.202100133
14. S. Zhu, J. Chen, Dual strategy with Li-ion solvation and solid electrolyte interphase for high Coulombic efficiency of lithium metal anode. Energy Storage Mater. **44**, 48–56 (2022). https://doi.org/10.1016/j.ensm.2021.10.007
15. T. Cai, Q. Sun, Z. Cao, Z. Ma, W. Wahyudi et al., Electrolyte additive-controlled interfacial models enabling stable antimony anodes for lithium-ion batteries. J. Phys. Chem. C **126**, 20302–20313 (2022). https://doi.org/10.1021/acs.jpcc.2c07094
16. R. Zhao, S. Shen, D. Chai, S. Tang, Y. Liao et al., Interface engineering enabling non-corrosive sulfonimide salt for 4.4 V class lithium batteries. J. Power Sour. **616**, 235125 (2024). https://doi.org/10.1016/j.jpowsour.2024.235125
17. Y.-W. Song, L. Shen, N. Yao, S. Feng, Q. Cheng et al., Anion-involved solvation structure of lithium polysulfides in lithium-sulfur batteries. Angew. Chem. Int. Ed. **63**, e202400343 (2024). https://doi.org/10.1002/anie.202400343
18. J. Chen, Y. Zhang, H. Lu, J. Ding, X. Wang et al., Electrolyte solvation chemistry to construct an anion-tuned interphase for stable high-temperature lithium metal batteries. eScience **3**, 100135 (2023). https://doi.org/10.1016/j.esci.2023.100135
19. J. Xu, V. Koverga, A. Phan, A. Min Li, N. Zhang et al., Revealing the anion-solvent interaction for ultralow temperature lithium metal batteries. Adv. Mater. **36**, e2306462 (2024). https://doi.org/10.1002/adma.202306462
20. J. Wu, Z. Gao, Y. Wang, X. Yang, Q. Liu et al., Electrostatic interaction tailored anion-rich solvation sheath stabilizing high-voltage lithium metal batteries. Nano-Micro Lett. **14**, 147 (2022). https://doi.org/10.1007/s40820-022-00896-4
21. R. Zhao, X. Li, Y. Si, S. Tang, W. Guo et al., $Cu(NO_3)_2$ as efficient electrolyte additive for 4 V class Li metal batteries with ultrahigh stability. Energy Storage Mater. **37**, 1–7 (2021). https://doi.org/10.1016/j.ensm.2021.01.030
22. J. Zhang, H. Zhang, S. Weng, R. Li, D. Lu et al., Multifunctional solvent molecule design enables high-voltage Li-ion batteries. Nat. Commun. **14**, 2211 (2023). https://doi.org/10.1038/s41467-023-37999-4
23. Q. Sun, Z. Gong, T. Zhang, J. Li, X. Zhu et al., Molecule-level multiscale design of nonflammable gel polymer electrolyte to build stable SEI/CEI for lithium metal battery. Nano-Micro Lett. **17**, 18 (2024). https://doi.org/10.1007/s40820-024-01508-z
24. N. Chen, M. Feng, C. Li, Y. Shang, Y. Ma et al., Anion-dominated conventional-concentrations electrolyte to improve low-temperature performance of lithium-ion batteries. Adv. Funct. Mater. **34**, 2400337 (2024). https://doi.org/10.1002/adfm.202400337
25. J.A. Weeks, J.N. Burrow, J. Diao, A.G. Paul-Orecchio, H.S. Srinivasan et al., *In situ* engineering of inorganic-rich solid electrolyte interphases *via* anion choice enables stable, lithium anodes. Adv. Mater. **36**, e2305645 (2024). https://doi.org/10.1002/adma.202305645
26. M. Qin, Z. Zeng, Q. Wu, F. Ma, Q. Liu et al., Microsolvating competition in Li^+ solvation structure affording PC-based electrolyte with fast kinetics for lithium-ion batteries. Adv. Funct. Mater. **34**, 2406357 (2024). https://doi.org/10.1002/adfm.202406357
27. G. Yang, S. Zhang, S. Weng, X. Li, X. Wang et al., Anionic effect on enhancing the stability of a solid electrolyte interphase film for lithium deposition on graphite. Nano Lett. **21**, 5316–5323 (2021). https://doi.org/10.1021/acs.nanolett.1c01436
28. H. Cheng, Q. Sun, L. Li, Y. Zou, Y. Wang et al., Emerging era of electrolyte solvation structure and interfacial model in batteries. ACS Energy Lett. **7**, 490–513 (2022). https://doi.org/10.1021/acsenergylett.1c02425
29. X. Zhu, J. Chen, G. Liu, Y. Mo, Y. Xie et al., Non-fluorinated cyclic ether-based electrolyte with quasi-conjugate effect for high-performance lithium metal batteries. Angew. Chem. Int. Ed. **64**, e202412859 (2025). https://doi.org/10.1002/anie.202412859
30. J. Chen, Z. Cheng, Y. Liao, L. Yuan, Z. Li et al., Selection of redox mediators for reactivating dead Li in lithium metal batteries. Adv. Energy Mater. **12**, 2201800 (2022). https://doi.org/10.1002/aenm.202201800
31. C.-B. Jin, X.-Q. Zhang, O.-W. Sheng, S.-Y. Sun, L.-P. Hou et al., Reclaiming inactive lithium with a triiodide/iodide redox couple for practical lithium metal batteries. Angew. Chem. Int. Ed. **60**, 22990–22995 (2021). https://doi.org/10.1002/anie.202110589
32. S. Qin, J. Zhang, M. Xu, P. Xu, J. Zou et al., Formulating self-repairing solid electrolyte interface *via* dynamic electric double layer for practical zinc ion batteries. Angew. Chem. Int. Ed. **63**, e202410422 (2024). https://doi.org/10.1002/anie.202410422
33. H. Wang, J. Zhang, H. Zhang, W. Li, M. Chen et al., Regulating interfacial structure enables high-voltage dilute ether

electrolytes. Cell Rep. Phys. Sci. **3**, 100919 (2022). https://doi.org/10.1016/j.xcrp.2022.100919

34. W. Zhang, Y. Lu, L. Wan, P. Zhou, Y. Xia et al., Engineering a passivating electric double layer for high performance lithium metal batteries. Nat. Commun. **13**, 2029 (2022). https://doi.org/10.1038/s41467-022-29761-z
35. D. Chai, H. Yan, X. Wang, X. Li, Y. Fu, Retuning solvating ability of ether solvent by anion chemistry toward 4.5 V class Li metal battery. Adv. Funct. Mater. **34**, 2310516 (2024). https://doi.org/10.1002/adfm.202310516
36. Z. Wang, F. Qi, L. Yin, Y. Shi, C. Sun et al., Lithium anodes: an anion-tuned solid electrolyte interphase with fast ion transfer kinetics for stable lithium anodes (adv. energy mater. 14/2020). Adv. Energy Mater. **10**, 2070063 (2020). https://doi.org/10.1002/aenm.202070063
37. S. Yuan, S. Cao, X. Chen, J. Wei, Z. Lv et al., Deshielding anions enable solvation chemistry control of $LiPF_6$-based electrolyte toward low-temperature lithium-ion batteries. Adv. Mater. **36**, e2311327 (2024). https://doi.org/10.1002/adma.202311327
38. K. Xu, C. Wang, Batteries: widening voltage windows. Nat. Energy **1**, 16161 (2016). https://doi.org/10.1038/nenergy.2016.161
39. L. Wu, F. Pei, D. Cheng, Y. Zhang, H. Cheng et al., Flame-retardant polyurethane-based solid-state polymer electrolytes enabled by covalent bonding for lithium metal batteries. Adv. Funct. Mater. **34**, 2310084 (2024). https://doi.org/10.1002/adfm.202310084
40. J.H. Yang, Y.K. Jeong, W. Kim, M.A. Lee, J.W. Choi et al., Dual flame-retardant mechanism-assisted suppression of thermal runaway in lithium metal batteries with improved electrochemical performances. Adv. Energy Mater. 2304366 (2024). https://doi.org/10.1002/aenm.202304366
41. Z. Huang, X. Li, Z. Chen, P. Li, X. Ji et al., Anion chemistry in energy storage devices. Nat. Rev. Chem. **7**, 616–631 (2023). https://doi.org/10.1038/s41570-023-00506-w
42. Z. Song, X. Wang, W. Feng, M. Armand, Z. Zhou et al., Designer anions for better rechargeable lithium batteries and beyond. Adv. Mater. **36**, 2310245 (2024). https://doi.org/10.1002/adma.202310245
43. B. Jagger, M. Pasta, Solid electrolyte interphases in lithium metal batteries. Joule **7**, 2228–2244 (2023). https://doi.org/10.1016/j.joule.2023.08.007
44. Y. Zhu, W. Li, L. Zhang, W. Fang, Q. Ruan et al., Electrode/electrolyte interphases in high-temperature batteries: a review. Energy Environ. Sci. **16**, 2825–2855 (2023). https://doi.org/10.1039/d3ee00439b
45. J. Popovic, The importance of electrode interfaces and interphases for rechargeable metal batteries. Nat. Commun. **12**, 6240 (2021). https://doi.org/10.1038/s41467-021-26481-8
46. W. Gu, G. Xue, Q. Dong, R. Yi, Y. Mao et al., Trimethoxyboroxine as an electrolyte additive to enhance the 4.5 V cycling performance of a Ni-rich layered oxide cathode. eScience **2**, 486–493 (2022). https://doi.org/10.1016/j.esci.2022.05.003
47. L. Lv, H. Zhang, D. Lu, Y. Yu, J. Qi et al., A low-concentration sulfone electrolyte enables high-voltage chemistry of lithium-ion batteries. Energy Mater. **2**, 200030 (2022). https://doi.org/10.20517/energymater.2022.38
48. F. Qiu, X. Li, H. Deng, D. Wang, X. Mu et al., A concentrated ternary-salts electrolyte for high reversible Li metal battery with slight excess Li. Adv. Energy Mater. **9**, 1803372 (2019). https://doi.org/10.1002/aenm.201803372
49. Q. Wu, M.T. McDowell, Y. Qi, Effect of the electric double layer (EDL) in multicomponent electrolyte reduction and solid electrolyte interphase (SEI) formation in lithium batteries. J. Am. Chem. Soc. **145**, 2473–2484 (2023). https://doi.org/10.1021/jacs.2c11807
50. Q. Zhao, S. Stalin, L.A. Archer, Stabilizing metal battery anodes through the design of solid electrolyte interphases. Joule **5**, 1119–1142 (2021). https://doi.org/10.1016/j.joule.2021.03.024
51. J.-F. Ding, R. Xu, C. Yan, B.-Q. Li, H. Yuan et al., A review on the failure and regulation of solid electrolyte interphase in lithium batteries. J. Energy Chem. **59**, 306–319 (2021). https://doi.org/10.1016/j.jechem.2020.11.016
52. H. Wang, J. Liu, J. He, S. Qi, M. Wu et al., Pseudo-concentrated electrolytes for lithium metal batteries. eScience **2**, 557–565 (2022). https://doi.org/10.1016/j.esci.2022.06.005
53. L. Chen, J. Lu, Y. Wang, P. He, S. Huang et al., Double-salt electrolyte for Li-ion batteries operated at elevated temperatures. Energy Storage Mater. **49**, 493–501 (2022). https://doi.org/10.1016/j.ensm.2022.04.036
54. H. Zhou, Z. Fang, J. Li, $LiPF_6$ and lithium difluoro(oxalato) borate/ethylene carbonate + dimethyl carbonate + ethyl(methyl)carbonate electrolyte for $Li_4Ti_5O_{12}$ anode. J. Power Sources **230**, 148–154 (2013). https://doi.org/10.1016/j.jpowsour.2012.11.060
55. R. Weber, M. Genovese, A.J. Louli, S. Hames, C. Martin et al., Long cycle life and dendrite-free lithium morphology in anode-free lithium pouch cells enabled by a dual-salt liquid electrolyte. Nat. Energy **4**, 683–689 (2019). https://doi.org/10.1038/s41560-019-0428-9
56. S. Yan, F. Liu, Y. Ou, H.-Y. Zhou, Y. Lu et al., Asymmetric trihalogenated aromatic lithium salt induced lithium halide rich interface for stable cycling of all-solid-state lithium batteries. ACS Nano **17**, 19398–19409 (2023). https://doi.org/10.1021/acsnano.3c07246
57. S. Wan, K. Song, J. Chen, S. Zhao, W. Ma et al., Reductive competition effect-derived solid electrolyte interphase with evenly scattered inorganics enabling ultrahigh rate and long-life span sodium metal batteries. J. Am. Chem. Soc. **145**, 21661–21671 (2023). https://doi.org/10.1021/jacs.3c08224
58. M. Yang, X. Chang, L. Wang, X. Wang, M. Gu et al., Interface modulation of metal sulfide anodes for long-cycle-life sodium-ion batteries. Adv. Mater. **35**, e2208705 (2023). https://doi.org/10.1002/adma.202208705
59. H. Jiang, Y. Han, C. Li, W. Sun, J. Zheng et al., Ultra-high voltage solid-state Li metal batteries enabled by *in situ* construction of cathode electrolyte interphase through synergistic dual-anion decomposition. Electrochim. Acta **457**, 142439 (2023). https://doi.org/10.1016/j.electacta.2023.142439

 https://doi.org/10.1007/s40820-024-01629-5

60. J. Zheng, M.H. Engelhard, D. Mei, S. Jiao, B.J. Polzin et al., Electrolyte additive enabled fast charging and stable cycling lithium metal batteries. Nat. Energy **2**, 17012 (2017). https://doi.org/10.1038/nenergy.2017.12
61. A. Fu, J. Lin, Z. Zhang, C. Xu, Y. Zou et al., Synergistical stabilization of Li metal anodes and $LiCoO_2$ cathodes in high-voltage Li||$LiCoO_2$ batteries by potassium selenocyanate (KSeCN) additive. ACS Energy Lett. **7**, 1364–1373 (2022). https://doi.org/10.1021/acsenergylett.2c00316
62. J. Chen, Y. Peng, Y. Yin, M. Liu, Z. Fang et al., High energy density Na-metal batteries enabled by a tailored carbonate-based electrolyte. Energy Environ. Sci. **15**, 3360–3368 (2022). https://doi.org/10.1039/D2EE01257J
63. C. Wang, X. Zhao, D. Li, C. Yan, Q. Zhang et al., Anion-modulated ion conductor with chain conformational transformation for stabilizing interfacial phase of high-voltage lithium metal batteries. Angew. Chem. Int. Ed. **63**, e202317856 (2024). https://doi.org/10.1002/anie.202317856
64. K. Dong, Y. Xu, J. Tan, M. Osenberg, F. Sun et al., Unravelling the mechanism of lithium nucleation and growth and the interaction with the solid electrolyte interface. ACS Energy Lett. **6**, 1719–1728 (2021). https://doi.org/10.1021/acsenergylett.1c00551
65. D. Aurbach, E. Zinigrad, Y. Cohen, H. Teller, A short review of failure mechanisms of lithium metal and lithiated graphite anodes in liquid electrolyte solutions. Solid State Ion. **148**, 405–416 (2002). https://doi.org/10.1016/S0167-2738(02)00080-2
66. D. Lin, Y. Liu, Y. Cui, Reviving the lithium metal anode for high-energy batteries. Nat. Nanotechnol. **12**, 194–206 (2017). https://doi.org/10.1038/nnano.2017.16
67. C. Fang, X. Wang, Y.S. Meng, Key issues hindering a practical lithium-metal anode. Trends Chem. **1**, 152–158 (2019). https://doi.org/10.1016/j.trechm.2019.02.015
68. C. Fang, J. Li, M. Zhang, Y. Zhang, F. Yang et al., Quantifying inactive lithium in lithium metal batteries. Nature **572**, 511–515 (2019). https://doi.org/10.1038/s41586-019-1481-z
69. C. Jin, T. Liu, O. Sheng, M. Li, T. Liu et al., Rejuvenating dead lithium supply in lithium metal anodes by iodine redox. Nat. Energy **6**, 378–387 (2021). https://doi.org/10.1038/s41560-021-00789-7
70. O. Sheng, H. Hu, T. Liu, Z. Ju, G. Lu et al., Interfacial and ionic modulation of poly (ethylene oxide) electrolyte *via* localized iodization to enable dendrite-free lithium metal batteries. Adv. Funct. Mater. **32**, 2111026 (2022). https://doi.org/10.1002/adfm.202111026
71. S. Ma, J. Zhao, Q. Gao, C. Song, H. Xiao et al., Breaking mass transport limitations by iodized polyacrylonitrile anodes for extremely fast-charging lithium-ion batteries. Angew. Chem. Int. Ed. **62**, e202315564 (2023). https://doi.org/10.1002/anie.202315564
72. Y. Xia, P. Zhou, X. Kong, J. Tian, W. Zhang et al., Designing an asymmetric ether-like lithium salt to enable fast-cycling high-energy lithium metal batteries. Nat. Energy **8**, 934–945 (2023). https://doi.org/10.1038/s41560-023-01282-z
73. P. Zhou, H. Zhou, Y. Xia, Q. Feng, X. Kong et al., Rational lithium salt molecule tuning for fast charging/discharging lithium metal battery. Angew. Chem. Int. Ed. **63**, e202316717 (2024). https://doi.org/10.1002/anie.202316717
74. Y. Qin, H. Wang, J. Zhou, R. Li, C. Jiang et al., Binding FSI^- to construct a self-healing SEI film for Li-metal batteries by *in situ* crosslinking vinyl ionic liquid. Angew. Chem. Int. Ed. **63**, e202402456 (2024). https://doi.org/10.1002/anie.202402456
75. J. Liu, J. Wang, Y. Ni, J. Liu, Y. Zhang et al., Tuning interphase chemistry to stabilize high-voltage $LiCoO_2$ cathode material *via* spinel coating. Angew. Chem. Int. Ed. **61**, e202207000 (2022). https://doi.org/10.1002/anie.202207000
76. S. Mao, J. Mao, Z. Shen, Q. Wu, S. Zhang et al., Specific adsorption-oxidation strategy in cathode inner Helmholtz plane enabling 4.6 V practical lithium-ion full cells. Nano Lett. **23**, 7014–7022 (2023). https://doi.org/10.1021/acs.nanolett.3c01700
77. J. Zhang, Y. Yan, X. Wang, Y. Cui, Z. Zhang et al., Bridging multiscale interfaces for developing ionically conductive high-voltage iron sulfate-containing sodium-based battery positive electrodes. Nat. Commun. **14**, 3701 (2023). https://doi.org/10.1038/s41467-023-39384-7
78. Z. Wen, W. Fang, F. Wang, H. Kang, S. Zhao et al., Dual-salt electrolyte additive enables high moisture tolerance and favorable electric double layer for lithium metal battery. Angew. Chem. Int. Ed. **63**, e202314876 (2024). https://doi.org/10.1002/anie.202314876
79. J. Ming, Z. Cao, W. Wahyudi, M. Li, P. Kumar et al., New insights on graphite anode stability in rechargeable batteries: Li ion coordination structures prevail over solid electrolyte interphases. ACS Energy Lett. **3**, 335–340 (2018). https://doi.org/10.1021/acsenergylett.7b01177
80. Z. Tian, Y. Zou, G. Liu, Y. Wang, J. Yin et al., Electrolyte solvation structure design for sodium ion batteries. Adv. Sci. **9**, 2201207 (2022). https://doi.org/10.1002/advs.202201207
81. N. Yao, S.-Y. Sun, X. Chen, X.-Q. Zhang, X. Shen et al., The anionic chemistry in regulating the reductive stability of electrolytes for lithium metal batteries. Angew. Chem. Int. Ed. **61**, e202210859 (2022). https://doi.org/10.1002/anie.202210859
82. S. Liu, C. Shu, Y. Yan, L. Ren, D. Du et al., Regulating solvation environment of Li ions via high donor number anions for high-performance Li-metal batteries. Chem. Eng. J. **450**, 138369 (2022). https://doi.org/10.1016/j.cej.2022.138369
83. H. Fu, X. Ye, Y. Zhang, Y. Zhong, X. Wang et al., Toward ultralow temperature lithium metal batteries: advancing the feasibility of 1, 3-dioxolane based localized high-concentration electrolytes *via* lithium nitrate. Adv. Energy Mater. **14**, 2401961 (2024). https://doi.org/10.1002/aenm.202401961
84. S. Kim, T.K. Lee, S.K. Kwak, N.-S. Choi, Solid electrolyte interphase layers by using lithiophilic and electrochemically active ionic additives for lithium metal anodes. ACS Energy Lett. **7**, 67–69 (2022). https://doi.org/10.1021/acsenergylett.1c02461
85. J. You, Q. Wang, R. Wei, L. Deng, Y. Hu et al., Boosting high-voltage practical lithium metal batteries with tailored additives. Nano-Micro Lett. **16**, 257 (2024). https://doi.org/10.1007/s40820-024-01479-1

86. D. Chai, Y. Zhu, C. Guan, T. Zhang, S. Tang et al., Achieving stable interphases toward lithium metal batteries by a dilute and anion-rich electrolyte. Energy Storage Mater. **62**, 102957 (2023). https://doi.org/10.1016/j.ensm.2023.102957
87. L. Zheng, F. Guo, T. Kang, Y. Fan, W. Gu et al., Stable lithium-carbon composite enabled by dual-salt additives. Nano-Micro Lett. **13**, 111 (2021). https://doi.org/10.1007/s40820-021-00633-3
88. Z. Jiang, T. Yang, C. Li, J. Zou, H. Yang et al., Synergistic additives enabling stable cycling of ether electrolyte in 4.4 V Ni-rich/Li metal batteries. Adv. Funct. Mater. **33**, 2306868 (2023). https://doi.org/10.1002/adfm.202306868
89. R. Zhao, X. Li, Y. Si, W. Guo, Y. Fu, Tuning solvation behavior of ester-based electrolytes toward highly stable lithium-metal batteries. ACS Appl. Mater. Interfaces **13**, 40582–40589 (2021). https://doi.org/10.1021/acsami.1c10279
90. X. Li, R. Zhao, Y. Fu, A. Manthiram, Nitrate additives for lithium batteries: mechanisms, applications, and prospects. eScience **1**, 108–123 (2021). https://doi.org/10.1016/j.esci.2021.12.006
91. Y. Zhu, X. Li, Y. Si, X. Zhang, P. Sang et al., Regulating dissolution chemistry of nitrates in carbonate electrolyte for high-stable lithium metal batteries. J. Energy Chem. **73**, 422–428 (2022). https://doi.org/10.1016/j.jechem.2022.06.046
92. M. Xia, M. Lin, G. Liu, Y. Cheng, T. Jiao et al., Stable cycling and fast charging of high-voltage lithium metal batteries enabled by functional solvation chemistry. Chem. Eng. J. **442**, 136351 (2022). https://doi.org/10.1016/j.cej.2022.136351
93. J. Jung, H. Chu, I. Kim, D.H. Lee, G. Doo et al., Confronting sulfur electrode passivation and Li metal electrode degradation in lithium-sulfur batteries using thiocyanate anion. Adv. Sci. **10**, e2301006 (2023). https://doi.org/10.1002/advs.202301006
94. Z. Jiang, C. Li, T. Yang, Y. Deng, J. Zou et al., Fluorine-free lithium metal batteries with a stable LiF-free solid electrolyte interphase. ACS Energy Lett. **9**, 1389–1396 (2024). https://doi.org/10.1021/acsenergylett.3c02724
95. J.-X. Chen, J.-H. Zhang, X.-Z. Fan, F.-F. Wang, W. Tang et al., Solvating lithium and tethering aluminium using dicoordination-strength anions for low-temperature lithium metal batteries. Energy Environ. Sci. **17**, 4036–4043 (2024). https://doi.org/10.1039/D3EE03809B
96. X. Chen, Q. Zhang, Atomic insights into the fundamental interactions in lithium battery electrolytes. Acc. Chem. Res. **53**, 1992–2002 (2020). https://doi.org/10.1021/acs.accounts.0c00412
97. K.W. Schroder, A.G. Dylla, L.D.C. Bishop, E.R. Kamilar, J. Saunders et al., Effects of solute-solvent hydrogen bonding on nonaqueous electrolyte structure. J. Phys. Chem. Lett. **6**, 2888–2891 (2015). https://doi.org/10.1021/acs.jpclett.5b01216
98. H. Li, Y. Kang, W. Wei, C. Yan, X. Ma et al., Branch-chain-rich diisopropyl ether with steric hindrance facilitates stable cycling of lithium batteries at –20 °C. Nano-Micro Lett. **16**, 197 (2024). https://doi.org/10.1007/s40820-024-01419-z
99. J. Wang, J. Zhang, J. Wu, M. Huang, L. Jia et al., Interfacial "single-atom-in-defects" catalysts accelerating Li^+ desolvation kinetics for long-lifespan lithium-metal batteries. Adv. Mater. **35**, e2302828 (2023). https://doi.org/10.1002/adma.202302828
100. Y. Huang, J. Geng, Z. Jiang, M. Ren, B. Wen et al., Solvation structure with enhanced anionic coordination for stable anodes in lithium-oxygen batteries. Angew. Chem. Int. Ed. **62**, e202306236 (2023). https://doi.org/10.1002/anie.202306236
101. X. Zhou, Y. Huang, B. Wen, Z. Yang, Z. Hao et al., Regulation of anion-Na^+ coordination chemistry in electrolyte solvates for low-temperature sodium-ion batteries. Proc. Natl. Acad. Sci. U.S.A. **121**, e2316914121 (2024). https://doi.org/10.1073/pnas.2316914121
102. H. Su, Z. Chen, M. Li, P. Bai, Y. Li et al., Achieving practical high-energy-density lithium-metal batteries by a dual-anion regulated electrolyte. Adv. Mater. **35**, e2301171 (2023). https://doi.org/10.1002/adma.202301171
103. P. Liang, H. Hu, Y. Dong, Z. Wang, K. Liu et al., Competitive coordination of ternary anions enabling fast Li-ion desolvation for low-temperature lithium metal batteries. Adv. Funct. Mater. **34**, 2309858 (2024). https://doi.org/10.1002/adfm.202309858
104. X. Ren, L. Zou, X. Cao, M.H. Engelhard, W. Liu et al., Enabling high-voltage lithium-metal batteries under practical conditions. Joule **3**, 1662–1676 (2019). https://doi.org/10.1016/j.joule.2019.05.006
105. C. Niu, H. Lee, S. Chen, Q. Li, J. Du et al., High-energy lithium metal pouch cells with limited anode swelling and long stable cycles. Nat. Energy **4**, 551–559 (2019). https://doi.org/10.1038/s41560-019-0390-6
106. Z. Wu, R. Li, S. Zhang, L. lv, T. Deng et al., Deciphering and modulating energetics of solvation structure enables aggressive high-voltage chemistry of Li metal batteries. Chem **9**, 650–664 (2023). https://doi.org/10.1016/j.chempr.2022.10.027
107. Y. Chen, Z. Yu, P. Rudnicki, H. Gong, Z. Huang et al., Steric effect tuned ion solvation enabling stable cycling of high-voltage lithium metal battery. J. Am. Chem. Soc. **143**, 18703–18713 (2021). https://doi.org/10.1021/jacs.1c09006
108. Y.-X. Yao, X. Chen, C. Yan, X.-Q. Zhang, W.-L. Cai et al., Regulating interfacial chemistry in lithium-ion batteries by a weakly solvating electrolyte. Angew. Chem. Int. Ed. **60**, 4090–4097 (2021). https://doi.org/10.1002/anie.202011482
109. Z. Jiang, J. Mo, C. Li, H. Li, Q. Zhang et al., Anion-regulated weakly solvating electrolytes for high-voltage lithium metal batteries. Energy Environ. Mater. **6**, 12440 (2023). https://doi.org/10.1002/eem2.12440
110. Y.-F. Tian, S.-J. Tan, Z.-Y. Lu, D.-X. Xu, H.-X. Chen et al., Insights into anion-solvent interactions to boost stable operation of ether-based electrolytes in pure-SiO_x||$LiNi_{0.8}Mn_{0.1}Co_{0.1}O_2$ full cells. Angew. Chem. Int. Ed. **62**, 202305988 (2023). https://doi.org/10.1002/anie.202305988
111. X. Min, C. Han, S. Zhang, J. Ma, N. Hu et al., Highly oxidative-resistant cyano-functionalized lithium borate salt for enhanced cycling performance of practical lithium-ion batteries. Angew. Chem. Int. Ed. **62**, e202302664 (2023). https://doi.org/10.1002/anie.202302664
112. D. Wu, C. Zhu, M. Wu, H. Wang, J. Huang et al., Highly oxidation-resistant electrolyte for 4.7 V sodium metal batteries

 https://doi.org/10.1007/s40820-024-01629-5

enabled by anion/cation solvation engineering. Angew. Chem. Int. Ed. **61**, e202214198 (2022). https://doi.org/10.1002/anie.202214198

113. S. Zhang, S. Li, Y. Lu, Designing safer lithium-based batteries with nonflammable electrolytes: a review. eScience **1**, 163–177 (2021). https://doi.org/10.1016/j.esci.2021.12.003
114. Z. Gao, S. Rao, T. Zhang, W. Li, X. Yang et al., Design strategies of flame-retardant additives for lithium ion electrolyte. J. Electrochem. Energy Convers. Storage **19**, 030910 (2022). https://doi.org/10.1115/1.4053968
115. R. He, K. Deng, D. Mo, X. Guan, Y. Hu et al., Active diluent-anion synergy strategy regulating nonflammable electrolytes for high-efficiency Li metal batteries. Angew. Chem. Int. Ed. **63**, e202317176 (2024). https://doi.org/10.1002/anie.202317176
116. Y. Zou, G. Liu, Y. Wang, Q. Li, Z. Ma et al., Intermolecular interactions mediated nonflammable electrolyte for high-voltage lithium metal batteries in wide temperature. Adv. Energy Mater. **13**, 2300443 (2023). https://doi.org/10.1002/aenm.202300443
117. D.-J. Yoo, Q. Liu, O. Cohen, M. Kim, K.A. Persson et al., Rational design of fluorinated electrolytes for low temperature lithium-ion batteries. Adv. Energy Mater. **13**, 2204182 (2023). https://doi.org/10.1002/aenm.202204182
118. M. Qin, Z. Zeng, F. Ma, C. Gu, X. Chen et al., Doping in solvation structure: enabling fluorinated carbonate electrolyte for high-voltage and high-safety lithium-ion batteries. ACS Energy Lett. **9**, 2536–2544 (2024). https://doi.org/10.1021/acsenergylett.4c00790
119. P. Xiao, Y. Zhao, Z. Piao, B. Li, G. Zhou et al., A nonflammable electrolyte for ultrahigh-voltage (4.8 V-class) Li||NCM811 cells with a wide temperature range of 100 °C. Energy Environ. Sci. **15**, 2435–2444 (2022). https://doi.org/10.1039/D1EE02959B
120. L. Tan, S. Chen, Y. Chen, J. Fan, D. Ruan et al., Intrinsic nonflammable ether electrolytes for ultrahigh-voltage lithium metal batteries enabled by chlorine functionality. Angew. Chem. Int. Ed. **61**, e202203693 (2022). https://doi.org/10.1002/anie.202203693
121. M. Zheng, X. Li, J. Sun, X. Wang, G. Liu et al., Research progress on chloride solid electrolytes for all-solid-state batteries. J. Power Sources **595**, 234051 (2024). https://doi.org/10.1016/j.jpowsour.2024.234051
122. D.H.S. Tan, A. Banerjee, Z. Chen, Y.S. Meng, From nanoscale interface characterization to sustainable energy storage using all-solid-state batteries. Nat. Nanotechnol. **15**, 170–180 (2020). https://doi.org/10.1038/s41565-020-0657-x
123. A. Manthiram, X. Yu, S. Wang, Lithium battery chemistries enabled by solid-state electrolytes. Nat. Rev. Mater. **2**, 16103 (2017). https://doi.org/10.1038/natrevmats.2016.103
124. C. Zuo, D. Dong, H. Wang, Y. Sun, Y.-C. Lu, Bromide-based nonflammable electrolyte for safe and long-life sodium metal batteries. Energy Environ. Sci. **17**, 791–799 (2024). https://doi.org/10.1039/d3ee03332e
125. Y. He, Y. Zhang, P. Yu, F. Ding, X. Li et al., Ion association tailoring SEI composition for Li metal anode protection. J. Energy Chem. **45**, 1–6 (2020). https://doi.org/10.1016/j.jechem.2019.09.033
126. Z. Jiang, Y. Deng, J. Mo, Q. Zhang, Z. Zeng et al., Switching reaction pathway of medium-concentration ether electrolytes to achieve 4.5 V lithium metal batteries. Nano Lett. **23**, 8481–8489 (2023). https://doi.org/10.1021/acs.nanolett.3c02013
127. Y. Yang, J. Wang, Z. Li, Z. Yang, B. Wang et al., Constructing LiF-dominated interphases with polymer interwoven outer layer enables long-term cycling of Si anodes. ACS Nano **18**, 7666–7676 (2024). https://doi.org/10.1021/acsnano.4c00998
128. S. Xue, J. Shang, X. Pu, H. Cheng, L. Zhang et al., Dual anionic doping strategy towards synergistic optimization of Co_9S_8 for fast and durable sodium storage. Energy Storage Mater. **55**, 33–41 (2023). https://doi.org/10.1016/j.ensm.2022.11.040
129. B. Wang, Y. Huang, Y. Wang, H. Wang, Synergistic solvation of anion: an effective strategy toward economical high-performance dual-ion battery. Adv. Funct. Mater. **33**, 2212287 (2023). https://doi.org/10.1002/adfm.202212287
130. H. Jiang, X. Han, X. Du, Z. Chen, C. Lu et al., A PF_6^-–permselective polymer electrolyte with anion solvation regulation enabling long-cycle dual-ion battery. Adv. Mater. **34**, e2108665 (2022). https://doi.org/10.1002/adma.202108665
131. X. Tong, X. Ou, N. Wu, H. Wang, J. Li et al., High oxidation potential ≈6.0 V of concentrated electrolyte toward high-performance dual-ion battery. Adv. Energy Mater. **11**, 2100151 (2021). https://doi.org/10.1002/aenm.202100151